

Distribution Agreement

In presenting this thesis or dissertation as a partial fulfillment of the requirements for an advanced degree from Emory University, I hereby grant to Emory University and its agents the non-exclusive license to archive, make accessible, and display my thesis or dissertation in whole or in part in all forms of media, now or hereafter known, including display on the world wide web. I understand that I may select some access restrictions as part of the online submission of this thesis or dissertation. I retain all ownership rights to the copyright of the thesis or dissertation. I also retain the right to use in future works (such as articles or books) all or part of this thesis or dissertation.

Signature:

Nicholas Eyrich

Date

Reactive Oxygen Species Signaling and Hypoxia-Independent Regulation of HIF1 α in
Sonic Hedgehog-Driven Medulloblastoma and Cerebellar Progenitor Proliferation

By

Nicholas Eyrich
Master of Science

Graduate Division of Biological and Biomedical Sciences
Cancer Biology and Translational Oncology

Anna M. Kenney, Ph.D.
Advisor

Malathy Shanmugam, Ph.D., M.S.
Committee Member

Keith D. Wilkinson, Ph.D.
Committee Member

Accepted:

Lisa A. Tedesco, Ph.D.
Dean of the James T. Laney School of Graduate Studies

Date

Reactive Oxygen Species Signaling and Hypoxia-Independent Regulation of HIF1 α in
Sonic Hedgehog-Driven Medulloblastoma and Cerebellar Progenitor Proliferation

By

Nicholas Eyrich
B.S., Emory University, 2016

Advisor: Anna M. Kenney, Ph.D.

An abstract of
A thesis submitted to the Faculty of the
James T. Laney School of Graduate Studies of Emory University
in partial fulfillment of the requirements for the degree of
Master of Science
in the Graduate Division of Biological and Biomedical Sciences
Cancer Biology and Translational Oncology
2017

Abstract

Reactive Oxygen Species Signaling and Hypoxia-Independent Regulation of HIF1 α in Sonic Hedgehog-Driven Medulloblastoma and Cerebellar Progenitor Proliferation

By Nicholas Eyrich

Medulloblastoma (MB) is the most common solid pediatric malignancy of the central nervous system. These tumors arise in the cerebellum and can be molecularly subdivided into 4 consensus subgroups, one of which is marked by amplification and activation of Sonic hedgehog (Shh) pathway components and downstream targets. This subclass is proposed to arise from oncogenic transformation of cerebellar granule neuron precursors (CGNPs), whose expansion during post-natal brain development is driven by and requires Shh pathway activation. CGNP cultures offer an excellent model system for studying Shh-driven MB, given its similarities with normal cerebellar development. Ex vivo tumor slice cultures also allow us to study MB cellular processes and pharmacological interventions with enhanced physiological relevance since tumor architecture and cell-cell interactions are preserved.

In addition to mitogens driving proliferation, it has been shown that low levels of intracellular reactive oxygen species (ROS) are required for proliferation through a myriad of mechanisms. In other cancers, increased ROS levels have been shown to affect other signaling events including the stabilization of Hypoxia-Inducible Factor-1-Alpha (HIF1 α) by interfering with prolyl hydroxylase's ability to tag HIF1 α for VHL-mediated degradation. HIF1 α , in addition to its oxygen-sensing role, has been implicated in the Warburg effect, which causes an increase in glycolytic activity and relative decrease in oxidative phosphorylation in oftentimes normoxic cancer cells. The current literature and preliminary studies led us to investigate potential sources of ROS within the NADPH Oxidase (Nox) family of proteins and possible consequences involving HIF1 α downstream of Shh. We've shown that HIF1 α is stabilized following Shh pathway induction, and under normoxic conditions, Nox activity is required to maintain a minimum level of ROS. Taken together, our findings suggest an axis mediated by Nox-generated ROS that helps understand hypoxia-independent regulation of HIF1 α in Shh medulloblastoma that could be contributing to tumor recurrence.

Reactive Oxygen Species Signaling and Hypoxia-Independent Regulation of HIF1 α in
Sonic Hedgehog-Driven Medulloblastoma and Cerebellar Progenitor Proliferation

By

Nicholas Eyrich
B.S., Emory University, 2016

Advisor: Anna M. Kenney, Ph.D.

A thesis submitted to the Faculty of the
James T. Laney School of Graduate Studies of Emory University
in partial fulfillment of the requirements for the degree of
Master of Science
in the Graduate Division of Biological and Biomedical Sciences
Cancer Biology and Translational Oncology
2017

Acknowledgements

The Kenney Lab:

Anna M. Kenney, Ph.D.

Chad Potts

Victor Maximov, Ph.D.

Anshu Malhotra, Ph.D.

Abhinav Dey, Ph.D.

James Felker, M.D.

Yun Wei

Hope Robinson

Thesis Committee:

Malathy Shanmugam, Ph.D., M.S.

Keith D. Wilkinson, Ph.D.

The Hambardzumyan Lab

Aflac

Laney Graduate School

GDBBS

Emory IMSD

Bill & Melinda Gates Foundation

Winship Cancer Institute

Table of Contents

<u>Introduction & Background</u>	<u>1</u>
Medulloblastoma Clinical Characteristics.....	2
Cerebellar Development and Shh Medulloblastoma.....	5
Hypoxia Inducible Factor-1-Alpha in Medulloblastoma and Its Hypoxia- Independent Regulation.....	8
Reactive Oxygen Species (ROS) in Cancer and HIF1 α Regulation.....	15
NADPH Oxidases: Key Sources of ROS in Cancer.....	17
Scope of the Thesis.....	21
<u>Materials and Methods</u>	<u>22</u>
Animal Studies.....	23
Cerebellar Granule Neuron Precursor Culture.....	23
Protein Collecting and Immunoblotting.....	24
<i>Ex Vivo</i> Organotypic SmoA1 Tumor Slice Culture.....	24
Immunofluorescence.....	25
Reactive Oxygen Species Assay	25
<u>Results</u>	<u>27</u>
HIF1 α Colocalizes with Stem Cell Markers in the MB Perivascular Niche.....	28
HIF1 α is Up-regulated in SmoA1 MB Tumors.....	30
HIF1 α Protein is Up-regulated in Shh-treated CGNPs.....	32
Shh Induces ROS Production in CGNPs.....	34
Antioxidant-Mediated Sequestering of ROS Reduces HIF1 α Protein Stabilization in Shh-treated CGNPs and in SmoA1 Medulloblastomas <i>Ex Vivo</i>	36

NADPH Oxidase Inhibition Reduces HIF1 α Protein Stabilization in Shh-treated CGNPs and in SmoA1 Medulloblastomas <i>Ex Vivo</i>	39
NADPH Oxidase 4 is Upregulated Downstream of Shh.....	39
<u>Discussion</u>	<u>42</u>
<u>References</u>	<u>48</u>

Table of Figures

Figure 1. Medulloblastoma and its Molecular Subgroups.....	3
Figure 2. Frequency of Each Molecular Subgroup of Medulloblastoma.....	4
Figure 3. Shh Signaling in Post-Natal Development of The Cerebellum.....	6
Figure 4. HIF-1 Transcriptional Activity and Its Correlation with Cancer Prognoses.....	10
Figure 5. Elevated HIF1 α at the Protein Level in Medulloblastoma compared to Normal Cerebellum.....	11
Figure 6. HIF1 α Expression in the Medulloblastoma Perivascular Niche.....	13
Figure 7. HIF1 α Protein Levels Increase in Shh-Treated CGNPs in an mTOR-dependent Manner.....	14
Figure 8. Factors that affect Cellular ROS Homeostasis and Pathway Signaling Relative to ROS Levels.....	16
Figure 9. Inducing ROS Increases Shh-Treated CGNP Proliferation and ROS Scavenging Attenuates Proliferation.....	16
Figure 10. Mitochondrial ROS Can Lead to HIF1 α Stabilization by Interfering with PHDs	18

Figure 11. Nox4 Structure and Screen of Potential ROS-Promoting Genes in Shh-Treated CGNPs.....	19
Figure 12. Elevated Levels of Nox4 Protein in Shh-Treated CGNPs and Mouse MB.....	20
Figure 13. HIF1 α Protein is up-regulated in SmoA1 MB.....	29
Figure 14. HIF1 α Colocalizes with Stem Cell Markers in the Medulloblastoma Perivascular Niche.....	31
Figure 15. HIF1 α Protein is Up-regulated in Shh-treated CGNPs.....	33
Figure 16. Shh Induces ROS Production in CGNPs.....	35
Figure 17. Immunoblot Analysis Following ROS Scavenging using NAC in Shh-Treated CGNPs and SmoA1 Medulloblastomas <i>Ex Vivo</i>	37
Figure 18. Immunoblot Analysis Following ROS Scavenging with GSH in Shh-Treated CGNPs and SmoA1 Medulloblastomas <i>Ex Vivo</i>	38
Figure 19. Immunoblot Analysis Following NADPH Oxidase Inhibition in Shh-Treated CGNPs and SmoA1 Medulloblastomas <i>Ex Vivo</i>	40
Figure 20. Nox4 Protein is Up-regulated in MB and Shh-treated CGNPs.....	41
Figure 21. Proposed Nox4—ROS—HIF1 α Model.....	46

Introduction & Background

MEDULLOBLASTOMA CLINICAL CHARACTERISTICS

Medulloblastoma (MB) is the most common solid pediatric malignancy of the central nervous system (CNS). MBs/primitive neuroectodermal tumors (PNETs) account for nearly 25% of pediatric CNS neoplasms (9-12). The current standard of care consists of surgery, chemotherapy, and craniospinal radiation. This harsh regimen results in a “cure” rate of approximately 70%, but survivors are beset with permanent, long-term side effects, including cognitive impairment, seizures, premature aging, and susceptibility to cancer (13). Identification of novel molecular targeted therapies is critical for the improved quality of life of survivors and reduced incidence of recurrence, which is lethal in medulloblastoma patients.

Medulloblastomas arise in the posterior fossa, or cerebellum (Fig. 1A), and can be divided into 4 genetically and histologically distinct subclasses (14). As noted in Fig. 1B, certain subgroups are marked by up-regulated expression of Sonic hedgehog (SHH) or Wnt pathway targets, and others are marked by amplification of c-myc (Group 3) or elevated expression of OTX2 and the presence of isochromosome 17q (Group 4).

Approximately 30% of all cases of medulloblastoma belong to the SHH subclass and has a specific prevalence among different age groups, as seen in Fig. 2 (2). In particular, MBs occurring in the youngest group mostly belong to the Shh subclass. Thus, elucidating processes underlying early cerebellar development and aberrant SHH signaling are crucial in understanding medulloblastoma formation and developing minimally-invasive targeted therapies.

A



B






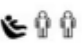



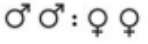

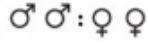

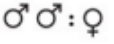

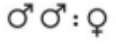



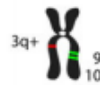

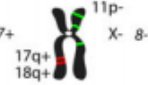
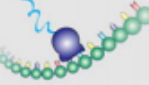
Molecular Subgroups of Medulloblastoma				
CONSENSUS	WNT	SHH	Group 3	Group 4
Cho (2010)	C6	C3	C1/C5	C2/C4
Northcott (2010)	WNT	SHH	Group C	Group D
Kool (2008)	A	B	E	C/D
Thompson (2006)	B	C', D	E, A	A, C
DEMOGRAPHICS				
Age Group:   				
Gender:  	 : 	 : 	 : 	 : 
CLINICAL FEATURES				
Histology	classic, rarely LCA	desmoplastic/nodular, classic, LCA	classic, LCA	classic, LCA
Metastasis	rarely M+	uncommonly M+	very frequently M+	frequently M+
Prognosis	very good	infants good, others intermediate	poor	intermediate
GENETICS				
	 CTNNB1 mutation	 PTCH1/SMO/SUFU mutation GLI2 amplification MYCN amplification	 i17q MYC amplification	 i17q CDK6 amplification MYCN amplification
GENE EXPRESSION				
	WNT signaling MYC +	SHH signaling MYCN +	Photoreceptor/GABAergic MYC +++	Neuronal/Glutamatergic minimal MYC / MYCN

Figure 1. Medulloblastoma (A) and its Molecular Subgroups (B): Medulloblastoma can be subdivided into the following subgroups based on respective genetic, prognostic, histologic, demographic, and gene expression signatures. This table includes affiliations with published papers related to medulloblastoma molecular subgrouping. Figure kindly borrowed from (2).

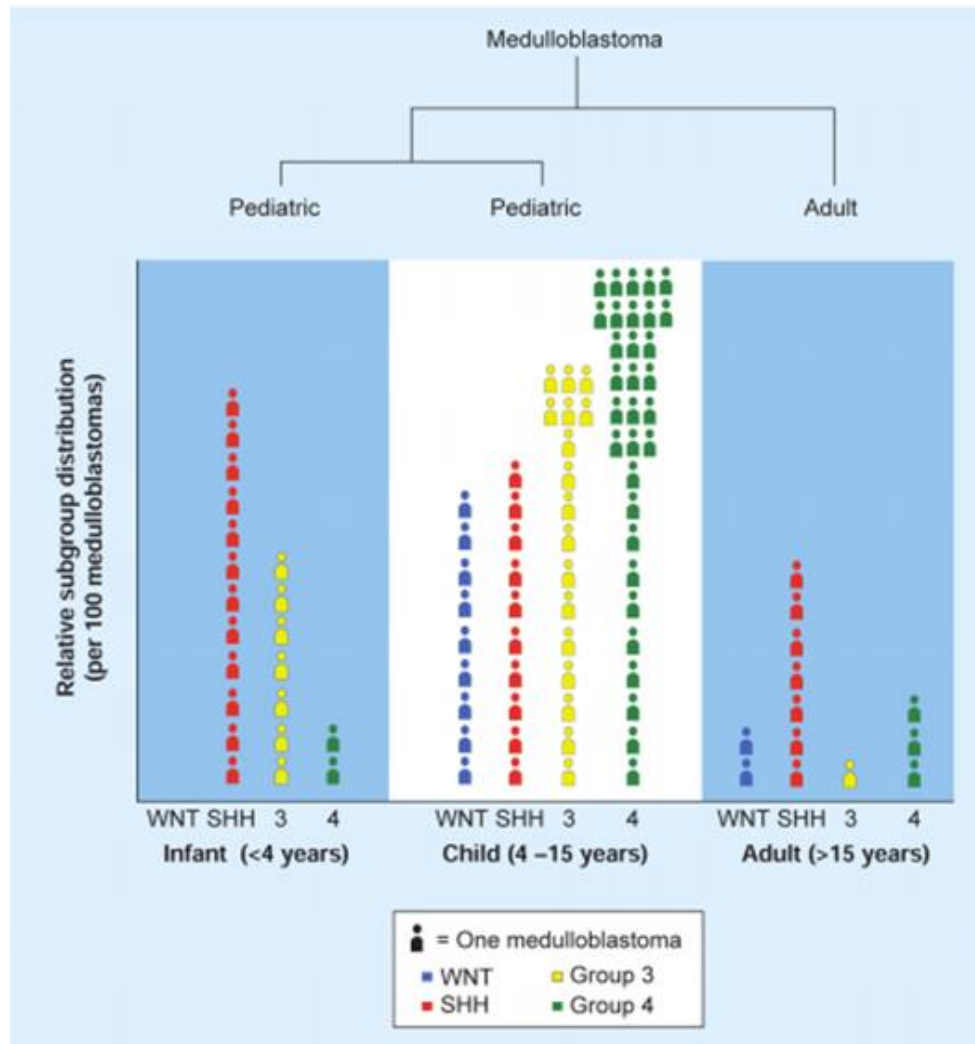


Figure 2. Frequency of Each Molecular Subgroup of Medulloblastoma: Approximately 60% of MB cases in infants (<4 years of age) bear the SHH molecular signature. This graph illustrates how different subclasses of MB more commonly arise in certain age groups. Figure kindly borrowed from (2).

CEREBELLAR DEVELOPMENT AND SHH MEDULLOBLASTOMA

In mice and humans, cerebellar development predominantly takes place postnatally (15). In the developing cerebellum, cerebellar granule neuron precursors (CGNPs), neural progenitors arising in the rhombic lip, are the proposed cells of origin for SHH driven MB (16-18). At birth, the cerebellum consists of three layers: the external granule layer (EGL) where CGNPs first reside, the molecular layer (MOL) where Purkinje neurons localize, and the internal granule layer (IGL), where CGNPs ultimately translocate. Shh is secreted by the Purkinje neurons (Fig. 3A), which is required for CGNPs to undergo rapid proliferation in the EGL before migrating through the MOL to the IGL, where they terminally differentiate and mature into glutamatergic interneurons (19, 20). In CGNPs, Shh ligand binding occurs at the 12-transmembrane domain receptor Patched (Ptch). In the absence of Shh, Ptch inhibits Smoothed (Smo), which is a 7-pass transmembrane protein. Shh binding to Ptch then releases Smo, resulting in Shh pathway activation and nuclear translocation of Gli family transcription factors (Fig. 3B). This activates target genes in CGNPs that drive proliferation and inhibit differentiation (18, 21, 22).

Conveniently, primary CGNPs derived from perinatal day 5 (P5) mice can be cultured and treated with exogenous Shh and insulin-like growth factor-2 (IGF2) to promote their survival and keep them in a proliferative state for approximately 72 hours. This system provides a powerful tool for isolating and studying Shh mitogenic signaling and interactions with other pathways (23, 24) including IGF, which cooperates with Shh at multiple levels during normal cerebellar development and in medulloblastoma (25-27).

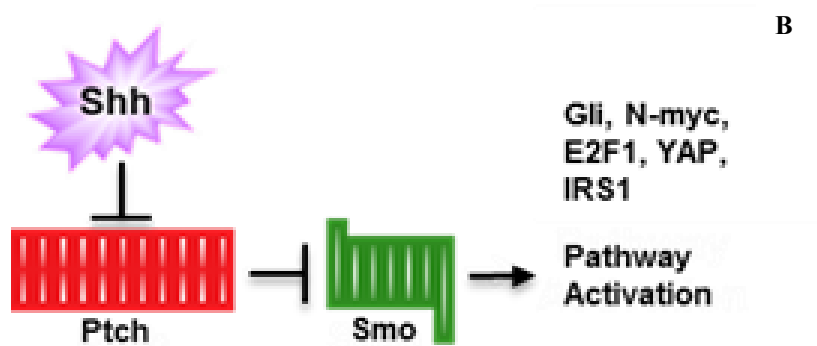
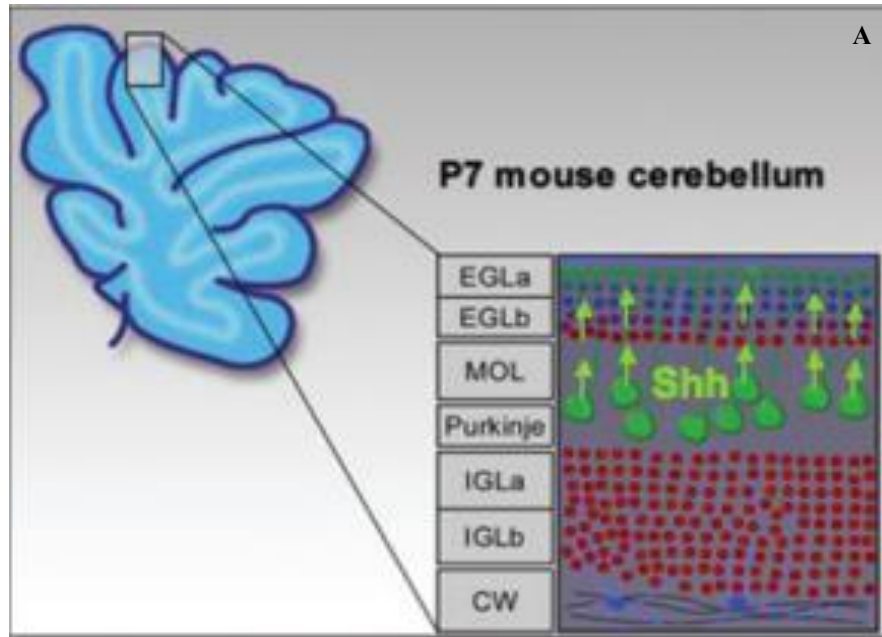


Figure 3. Shh Signaling in Post-Natal Development of The Cerebellum: (A) CGNPs originally reside in the EGL and undergo Shh-dependent rapid proliferation. Shh is produced by Purkinje neurons in the MOL. CGNPs then translocate to the IGL, where they differentiate into glutamatergic interneurons. Borrowed from (4). (B) A schematic of Shh ligand binding and a brief outline of downstream effectors. Figures kindly modified from (8).

CGNP cultures allow for the *in vitro* study of aberrant Shh signaling that takes place in MB formation and could foster identification of potential therapeutic targets downstream of Shh.

Additionally, we can reliably recapitulate Shh MB in mice. These genetically engineered mice, referred to as SmoA1 mice, express a constitutively active Smoothed allele under the control of the NeuroD2 promoter (28, 29), thereby activating aberrant Shh signaling in the developing mouse cerebellum. We also possess a sophisticated SmoA1 mouse model coupled with the Math1-Green Fluorescent Protein (GFP) reporter, allowing SmoA1 tumor cells to express GFP, which facilitates resection and allows for clear visualization of metastasis (see materials & methods).

As mentioned, Shh has been shown to cooperate with the IGF pathway, which occurs through regulation of insulin receptor substrate 1 (IRS1) and the kinase mammalian target of rapamycin (mTOR), which drive CGNP proliferation and promote Shh medulloblastoma cell survival (30-33). Of note, mTOR is involved in many cellular functions, including ribosomal biogenesis, nutrient metabolism, early neuronal development, and integration of signals from a myriad of cellular factors (34-37). Shh regulates IRS1 stability which promotes IGF-mediated activation of mTOR in Shh medulloblastoma (8, 27, 38, 39). Therapeutic strategies targeting mTOR in medulloblastoma patients have also been explored and shown to be promising (40). Furthermore, Shh promotes activity of eukaryotic initiation factor 4E (eIF4E) to increase mRNA translation in CGNPs (41), adding to their proliferative capacity. Additionally, Shh mitogenic signaling is involved in metabolic reprogramming of proliferating CGNPs and SmoA1 tumors. In congruence with the Warburg effect, increased levels of glycolytic

enzymes have been observed in both systems (42, 43) accompanied by an increase in lipogenesis (41).

HYPOXIA INDUCIBLE FACTOR-1-ALPHA IN MEDULLOBLASTOMA AND ITS HYPOXIA-INDEPENDENT REGULATION

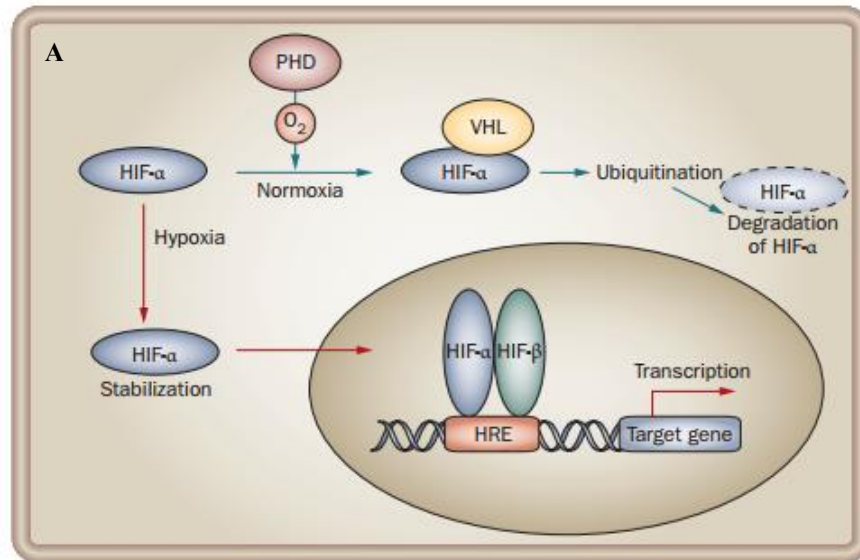
Hypoxia Inducible Factor-1 (HIF-1) is a heterodimeric helix-loop-helix transcription factor which acts as a master regulator of gene expression in response to tumor oxidative stress across a broad array of cancers (6, 44, 45). Transcriptionally active HIF-1 consists of an oxygen-regulated alpha subunit, and a constitutively expressed beta subunit (46).

HIF-1-driven gene expression has been extensively studied in cancer and regulates oxidative stress-induced metabolic reprogramming (increased glycolysis), stemness, angiogenesis, cell survival, invasion, metastasis, and therapy resistance (47-53). The degradation of Hypoxia Inducible Factor-1-Alpha (HIF1 α) is the rate-limiting step in HIF-1 activation (Fig. 4A), and its stabilization has been an attractive area of research and a target for the development of novel cancer therapies (54, 55). Increased HIF1 α expression is correlated with poor prognosis among a variety of malignancies (Fig. 4B). HIF1 α has also been shown to play a role in radiation resistance of MB and other cancers, specifically in the tumor perivascular niche (PVN) where tumor stem cells responsible for driving recurrence reside (56-62).

Conventionally, HIF1 α is degraded under normoxic conditions. In the presence of adequate oxygen levels, prolyl hydroxylases (PHDs) hydroxylate HIF1 α at two proline sites (P402 and P564). Hydroxy-HIF1 α is then sequestered and marked for proteasomal

degradation by the Von Hippel-Lindau (VHL) complex, a tumor suppressive E3 ubiquitin ligase (3, 46). HIF1 α is stabilized under hypoxic conditions when its hydroxylation-driven degradation is inhibited. Upon stabilization, it translocates to the nucleus where it complexes with HIF1 β and coactivators P300/CBP at the hypoxia responsive element (HRE; consensus sequence: G/ACGTG) to induce expression of cellular reprogramming genes mentioned previously. HIF1 α also promotes expression of PHDs as part of a negative feedback loop, which in turn marks HIF1 α for degradation upon return to normoxia (63).

As is the case in other cancers, HIF1 α presented as an attractive area of investigation within the Shh subclass of MB given its known pro-proliferative/survival signaling as well as its role in early mammalian development and cancer-promoting metabolic reprogramming. Our preliminary data indicate that HIF1 α is upregulated in MB tumor tissue compared to the neighboring normal cerebellum (CB) at the protein level, (Fig. 5A), but not at the mRNA level (Fig. 5B). In accordance, *in vivo* treatment of SmoA1 tumor-bearing mice with a brain-penetrant mTOR inhibitor, CCI-779 (temsirolimus; Wyeth-Ayerst/Pfizer), increased their survival (data not shown) and resulted in a decrease in HIF1 α levels and downstream glycolytic enzymes (Fig. 5A). Interestingly, mTOR has been implicated in tumorigenic responses to oxidative stress and shown to regulate HIF1 α translation leading to metabolic reprogramming and cancer survival/progression (64-67). Additionally, diminishing HIF1 α levels by mTOR inhibition further suggests that regulation of HIF1 α stability in Shh-driven MB occurs post-transcriptionally.



B

Cancer type	Prognosis		Refs
	HIF1α expression	HIF2α expression	
Astrocytoma	Poor	Poor	161,162
Bladder	Poor	ND	163
Breast	Poor	Poor	164,165
Cervical	Poor	Poor [†]	166,167
Colorectal	Poor	Poor	168
Gastric	Poor	NC	169,170
	Poor	ND	171
GIST	Poor	ND	172
Glioblastoma	ND	Poor	162
Glioma	NC [‡]	Poor [‡]	69
Head and neck	Poor	Poor	173,174
Hepatocellular	ND	Poor	175
NSCLC	Poor	Poor	176
	Poor	ND	177
	NC	Poor	178
Melanoma	Poor	Poor	179
Neuroblastoma	Favourable	Poor	180
Ovarian	Poor	ND	181
	Poor	Poor [‡]	182
Pancreatic	Poor	ND	183,184
Prostate	Poor	Poor [‡]	185
RCC	Favourable	ND	186
	Poor	ND	187

Figure 4. HIF-1 Transcriptional Activity and Its Correlation with Cancer Prognoses: (A) A schematic outlining the canonical steps in HIF1α degradation under normoxia and its hypoxia-induced stabilization pathway components. Borrowed from (3). (B) Evidence to support a correlation between HIF1α expression and poor prognosis among numerous human cancer types. Figure kindly borrowed from (6).

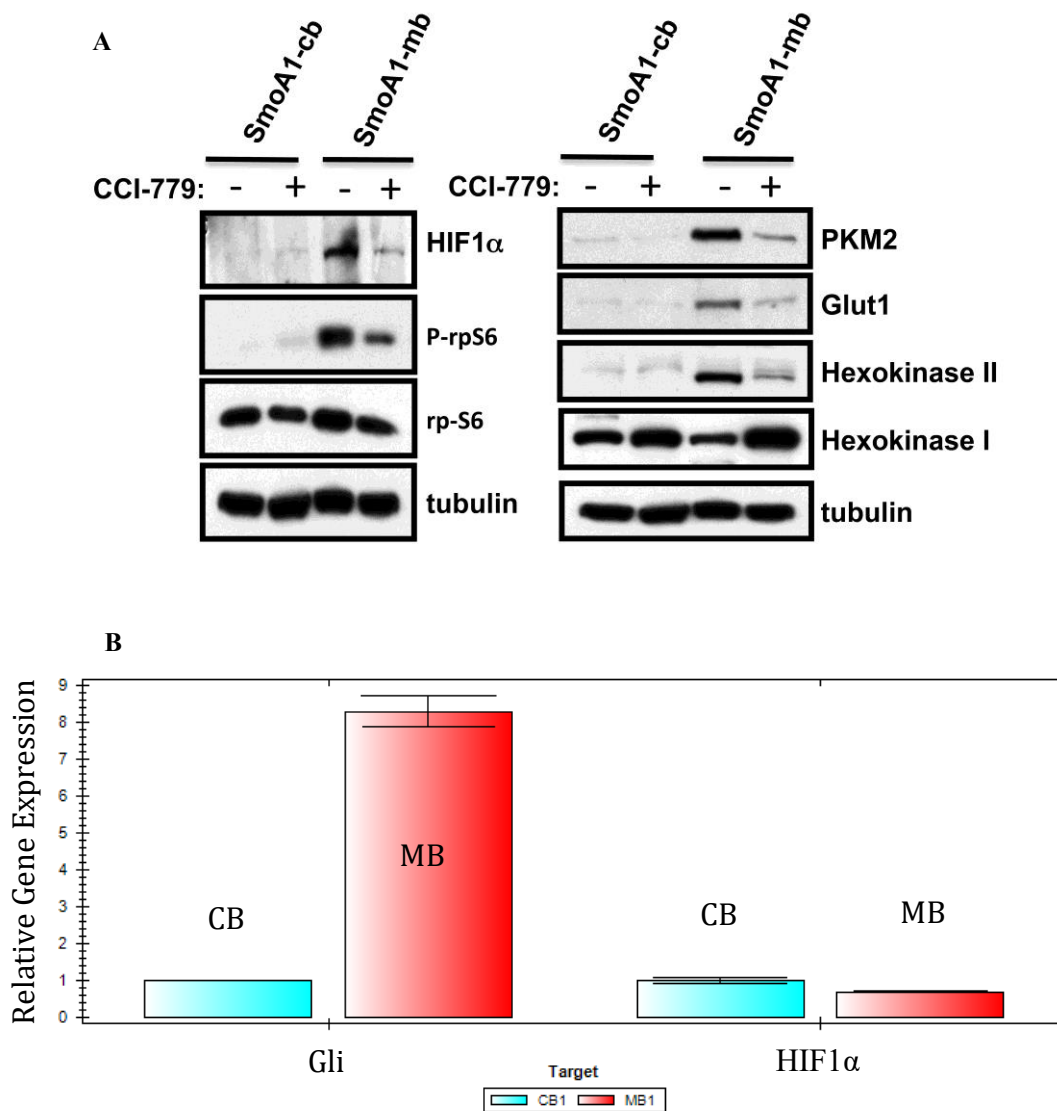


Figure 5. Elevated HIF1 α at the Protein Level in Medulloblastoma Compared to Normal Cerebellum (A) Western blot analysis of tissue samples from normal cerebella (CB) compared to SmoA1 medulloblastoma (MB) treated with vehicle or mTOR inhibitor CCI-779. Note reduction in HIF1 α levels and of subsequent glycolytic enzymes. (B) qPCR analysis of HIF1 α gene expression in CB (blue) compared to MB (red) from SmoA1 mice. N=3. (Bobby Bhatia, Kenney Lab, Unpublished data).

Follow-up studies in the Kenney lab aimed to characterize HIF1 α localization within SHH MB and its conferral of adaptive characteristics. Interestingly, immunofluorescence of SmoA1 tumor sections revealed colocalization of HIF1 α and nestin-positive neural stem-like cells within the MB PVN (Fig. 6A). This subset of cells, as previously described, has been found to resist radiation and drive lethal tumor recurrence. We also observed concurrent expression of PHD2 and PHD3 in the MB PVN (Fig. 6B-6C, respectively), which are known to be upregulated by HIF1 α as it attempts to mediate its own degradation.

With these seminal findings, we then investigated whether the observed up-regulation of HIF1 α in SmoA1 tumors is downstream of Shh signaling using our *in vitro* CGNP model system. Exogenous administration of Shh to CGNPs, the putative cells of origin for Shh MB, mimics the signaling events that take place in early tumor formation. Notably, our preliminary studies found that constitutive Shh pathway signaling in CGNPs resulted in increased levels of HIF1 α at the protein level (Fig. 7A) but not at the mRNA level (Fig. 7B). Similar to the MB tissue experiments described earlier in Fig. 5, inhibiting mTOR (mTORC1) with rapamycin diminishes HIF1 α protein levels (Fig. 7C), which supports Shh-induced HIF1 α stabilization being a post-transcriptional process. Furthermore, Shh-induced HIF1 α is transcriptionally active, as there is increased glycolysis and expression of angiogenic factors such as vascular endothelial growth factor (VEGF) (41). At this point, the Kenney lab had gathered striking evidence of Shh-dependent HIF1 α activity under oxygen-rich microenvironments, in the MB PVN and CGNP culture (actually hyperoxic compared to physiological standards). In both model systems, up-regulation of prolyl hydroxylases accompanies HIF1 α induction, but we have

been unable to detect HIF1 α hydroxylation using a number of methods, indicating that Shh-dependent HIF1 α stabilization in Shh-treated CGNPs and MB may be a result of inhibition of PHD activity. This drove forth experimentation to unravel the possible hypoxia-independent mechanisms that could be interfering with hydroxylation of HIF1 α , conferring its stability and transcriptional activity in Shh MB and its Shh-driven precursors.

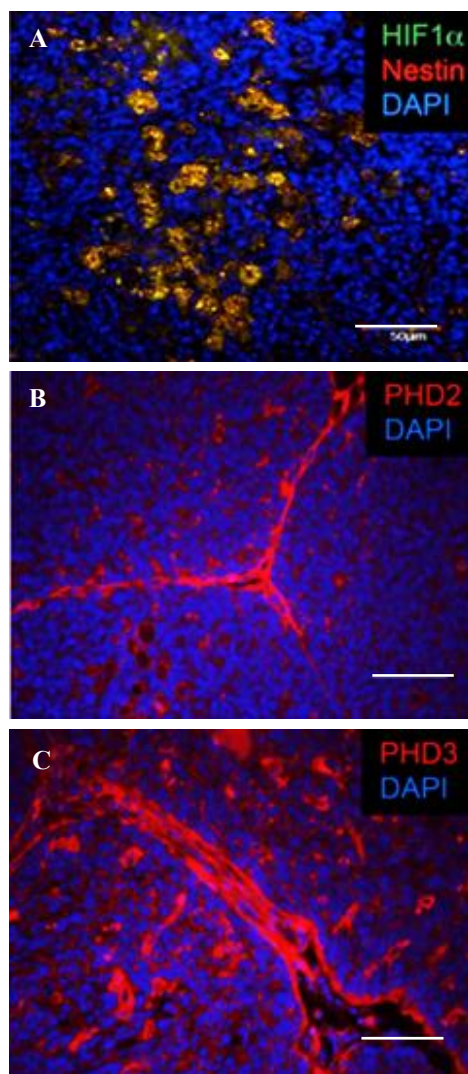


Figure 6. HIF1 α Expression in the Medulloblastoma Perivascular Niche: (A) HIF1 α co-localizes with nestin-positive cells, and its targets PHD2 (B) and PHD3 (C) are also found in the PVN. Scale Bar = 50 μ m. N=3. (Bobby Bhatia, Kenney Lab, Unpublished data).

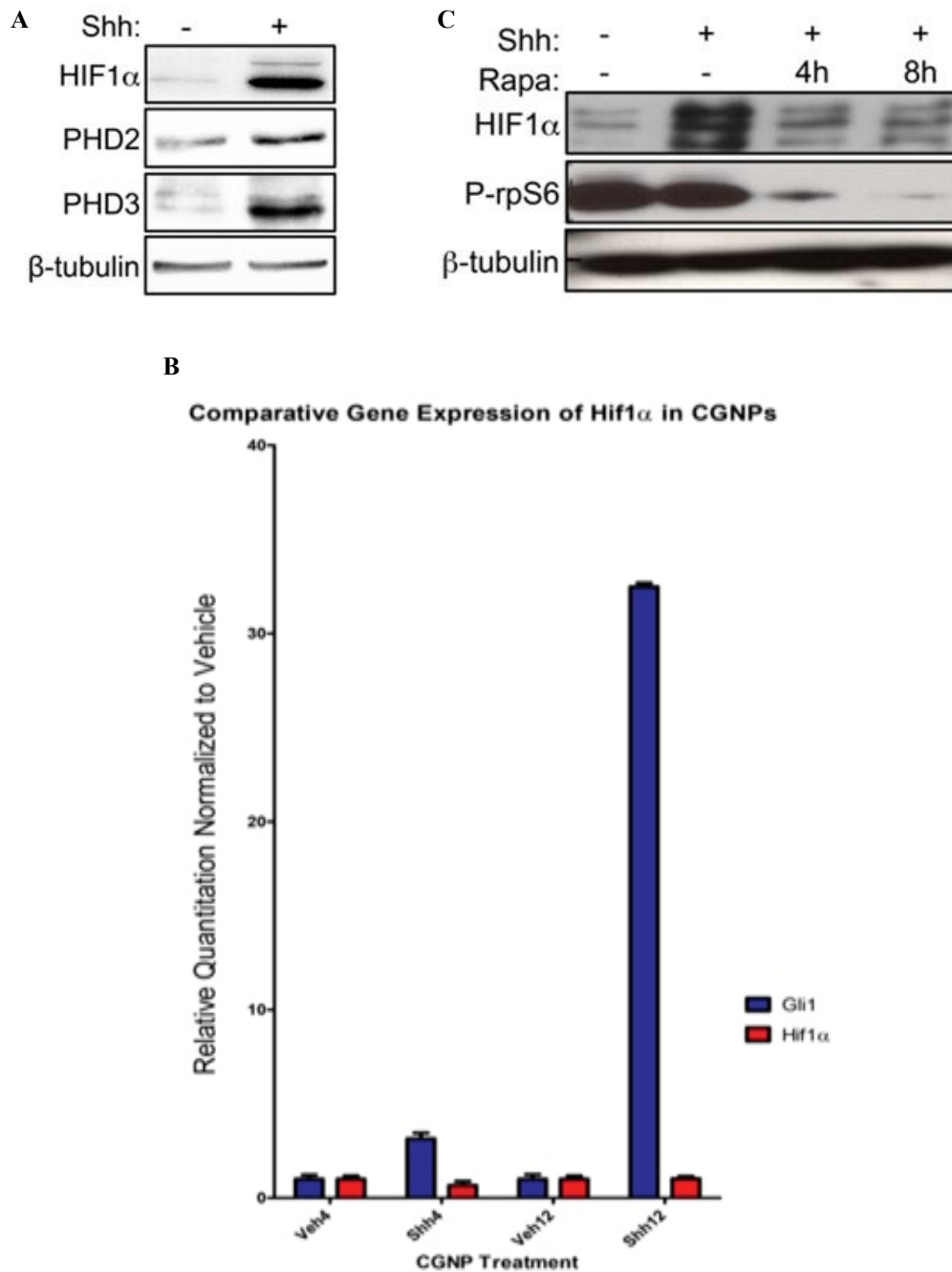


Figure 7. HIF1 α Protein Levels Increase in Shh-Treated CGNPs in an mTOR-dependent Manner: (A) Immunoblotting showing HIF1 α up-regulation in Shh-treated CGNPs. (B) qPCR quantification showing insignificant HIF1 α mRNA up-regulation (Red) (Gli1, blue). (C) Rapamycin treatment (10nM) reduces HIF1 α levels in Shh-treated CGNPs. N=3. (Bobby Bhatia, Kenney Lab, Unpublished data).

REACTIVE OXYGEN SPECIES (ROS) IN CANCER AND HIF1 α REGULATION

Reactive oxygen species (ROS) are highly reactive molecules or radicals that have one unpaired electron in their outermost shell. They can be assigned to one of two groups: free oxygen radicals or non-radical ROS, with superoxide ($O_2^{\bullet-}$) and hydrogen peroxide (H_2O_2) being the most well-known, respectively (5). ROS are commonly generated by the cell as a metabolic byproduct and generated for different reductive processes. ROS signaling events have been reported to influence various acquired characteristics (Fig. 8) across a wide range of cancers including, but not limited to, tumor stemness, cell morphology, proliferation, motility, survival, metabolic reprogramming, cell-cell adhesion, and angiogenesis (5, 68-72).

In preliminary studies, we cultured CGNPs in the presence of Shh plus the ROS inducer tert-Butyl hydroperoxide (tBHP) or the ROS scavenger lipoic acid (LA). Using Ki67 immunostaining to detect proliferation we found that ROS induction increased proliferation in Shh-treated CGNPs whereas ROS inhibition reduced levels of proliferation (Fig. 9). ROS homeostasis has also been shown to be an intricate and highly regulated process in the maintenance of tumor stem cells (73, 74), further suggesting that ROS could be playing a role in Shh-treated CGNP HIF1 α stability and potentially influencing tumor cell stemness in the MB PVN.

In conjunction with our previous findings that Shh acts upstream of HIF1 α , it has been shown that PHDs can be inhibited by ROS, from the mitochondria in particular,

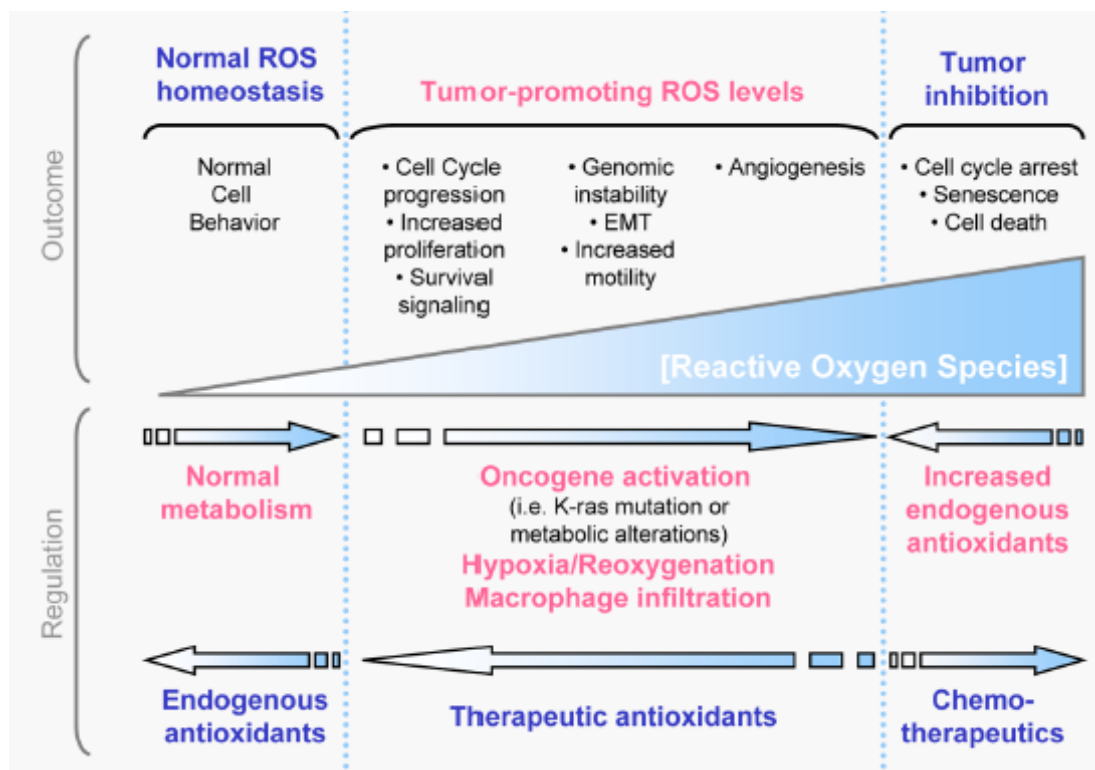


Figure 8. Factors that affect Cellular ROS Homeostasis and Pathway Signaling Relative to ROS Levels: (A) A schematic of endogenous and exogenous influences on ROS production and sequestering. As ROS levels increase they attain tumor-promoting qualities. Extremely high amounts of ROS can lead to tumor inhibition and cell death. Figure kindly borrowed from (5).

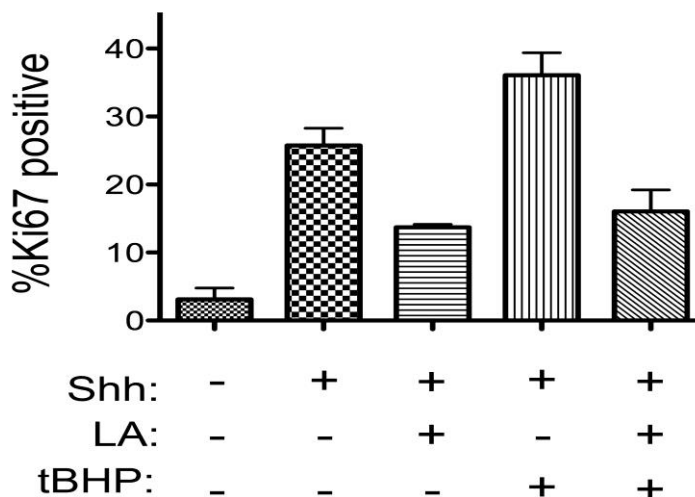


Figure 9. Inducing ROS Increases Shh-Treated CGNP Proliferation and ROS Scavenging Attenuates Proliferation: Quantification of immunofluorescence staining using the proliferation marker Ki67 in CGNPs treated with Shh, plus tBHP (ROS inducing agent) or the antioxidant lipoic acid (LA); N=1. (Chad Potts, Kenney Lab, Unpublished data).

leading to HIF1 α stabilization (Fig. 10) independent of hypoxia (75-81). PHD-mediated hydroxylation of HIF1 α requires ferrous iron (Fe²⁺), and elevated ROS within the cell favors the conversion to ferric iron (Fe³⁺), which hinders signaling for degradation (7). ROS has also been implicated in tumor angiogenesis via VEGF and a metabolic shift toward glycolysis, both being established processes linked to HIF1 α transcriptional activity (82, 83). Taken together, these observations suggest a role for ROS signaling in Shh-driven CGNP proliferation and medulloblastoma, and that this role could include HIF1 α stabilization.

NADPH OXIDASES: KEY SOURCES OF ROS IN CANCER

The NADPH Oxidase (Nox) family of transmembrane proteins are potential regulators of PHD-inhibiting ROS within Shh MB given their well-established enzymatic production of cellular ROS and the extensive literature describing them as essential modulators of signal transduction across various cell types (84, 85). Examples of signaling pathways modified by Nox-derived ROS include hormone synthesis, redox signaling, host defense mechanisms (phagocytes), cellular matrix modification and others that have yet to be characterized (1, 86). As previously mentioned, ROS production can occur as a metabolic byproduct, but the Nox family of proteins uniquely produce ROS as their primary function (86). Currently, 7 Nox homologues have been identified in humans, they vary in the amount/type/timing of ROS production and their organ-specific expression (1).

Nox4 (Fig. 11A) is the only member of the Nox family to display constitutive activation (87-89). Although Nox4, like other members of the Nox family, does interact

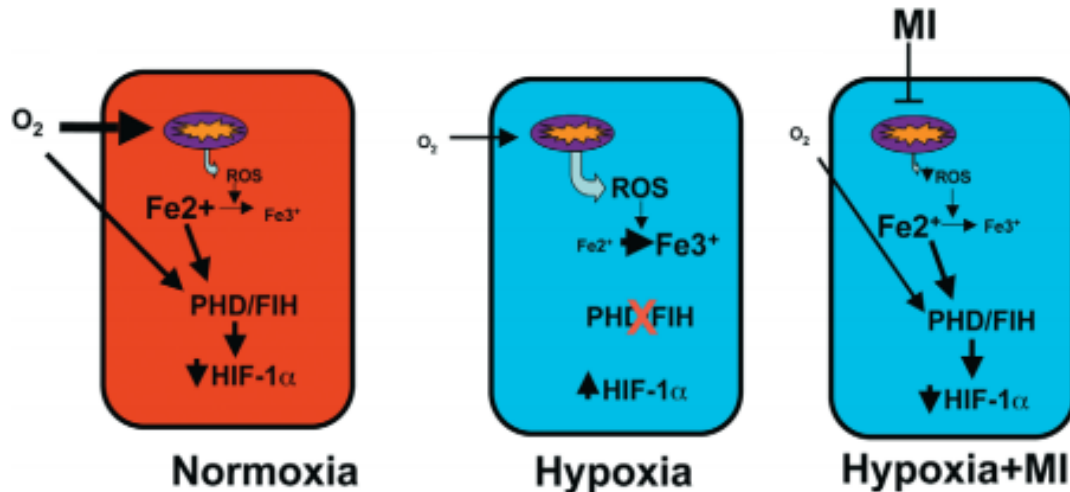


Figure 10. Mitochondrial ROS Can Lead to HIF1 α Stabilization by Interfering with PHDs: Under normoxia, basal ROS levels and adequate oxygen allow for HIF1 α hydroxylation/degradation. Increased ROS favors iron in the ferric state, thus promoting HIF1 α stability. Reducing ROS by mitochondrial inhibition (MI) leads to increased HIF1 α degradation even under hypoxia. Of note, this process is not static as basal cell metabolic demands combined with the degree and duration of hypoxia the come into play as well. Figure kindly borrowed from (7).

with the transmembrane coactivator p22phox, its ability to produce ROS is uniquely not altered by point mutations p22phox's proline-rich region that block binding (90). The increase in NADPH levels that generally accompanies actively proliferating cancer cells made Nox4 of interest to us in the context of Shh-driven MB. A qPCR screen of literature-based ROS-related candidate genes in Shh-treated CGNPs displayed a marked increase in Nox4 gene expression (Fig. 11B), which persuaded us to continue to pursue Nox4.

Follow-up studies indicated that Shh upregulates Nox4 in CGNPs in a Smo-dependent manner (Fig. 12A), and there is a notable increase of Nox4 protein in MB compared to neighboring normal cerebellar tissue (Fig. 12B). Of note, PHD inhibition/HIF1 α accumulation resulting from Nox activity has been studied in other cancer models (91). Extensive work has been done analyzing the relationship between Nox4 and HIF1 α -

driven tumor progression (84, 85, 92, 93). We became very interested in investigating a therapeutically relevant relationship between Nox4 and HIF1 α because of their concomitant upregulation downstream of Shh; Nox4 and HIF1 α have both been found in the tumor vasculature (94), and the link between the two remains poorly understood in Shh-driven medulloblastoma.

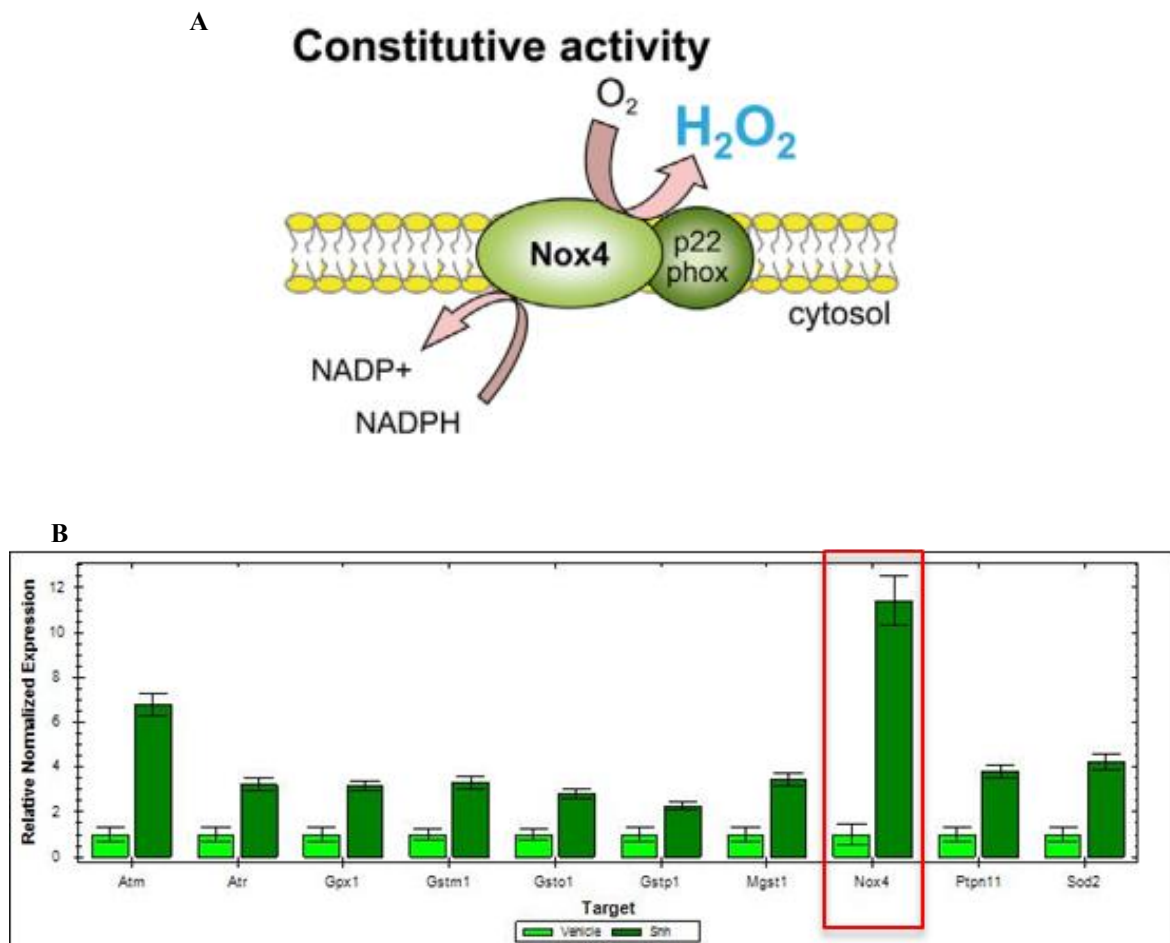


Figure 11. Nox4 Structure and Screen of Potential ROS-Promoting Genes in Shh-Treated CGNPs (A) The enzymatic composition and mechanism of action of Nox4. Figure kindly borrowed from (1) (B) qPCR of ROS-related candidate genes indicating a significant increase in Nox4 expression in CGNPs receiving exogenous Shh. Vehicle treatment: light green; Shh treatment: dark green. N=1. (Chad Potts, Kenney Lab, Unpublished data).

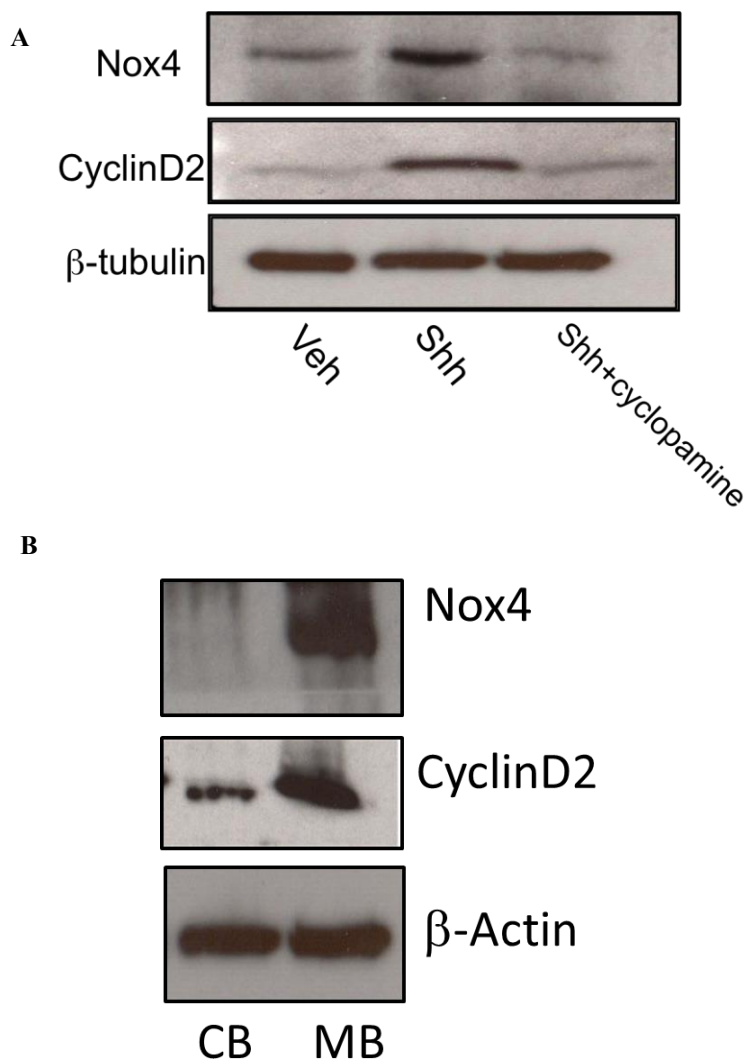


Figure 12. Elevated Levels of Nox4 Protein in Shh-Treated CGNPs and Mouse MB: (A) Immunoblot analysis showing that Shh signaling in CGNPs results in upregulated Nox4 protein levels. After treating with Shh, inhibition of the pathway using the Smo antagonist cyclopamine restored Nox4 levels back to similar levels as vehicle-treated CGNPs. (B) Immunoblot analysis demonstrating elevated Nox4 protein levels in SmoA1 tumor tissue compared to adjacent normal cerebellum. Increased Cyclin D2 protein denotes active cellular proliferation and serves as confirmation of Shh pathway activation in CGNPs. N=1. (Chad Potts, Kenney Lab, Unpublished data).

SCOPE OF THE THESIS

Given the overwhelming evidence for therapeutically targeting HIF1 α signaling in many cancers, we wanted to understand how HIF1 α is regulated in Shh medulloblastoma. Our preliminary findings, complemented by the current literature, strongly indicate that Shh-induced HIF1 α oncogenic signaling in CGNPs and SmoA1 tumors occurs under normoxia and results in increased transcription.

We hypothesize that inhibition of PHD activity, resulting in hypoxia-independent HIF1 α stabilization and transactivation, is regulated by Nox-produced ROS in Shh-treated CGNPs and in the Shh medulloblastoma perivascular niche. This thesis addresses our hypothesis by: (i) recapitulating prior findings from the Kenney lab outlined above to attest to their reproducibility and build statistical strength; (ii) optimizing a ROS assay to quantify intracellular ROS levels following constitutive Shh signaling or other pharmacological intervention; and (iii) testing if sequestering ROS and/or inhibiting Nox production of ROS restores hydroxylation and degradation of HIF1 α downstream of Shh.

This work elucidates a possible mechanism by which CGNP oncogenic transformation occurs as a result of aberrant Shh signaling, and begins to unravel HIF1 α regulation in the medulloblastoma PVN, where radiation-surviving and tumor-repopulating stem cells reside.

Materials and Methods

Animal Studies

Harvest of cerebellar granule neuron precursors from neonatal mice and preparation of cerebella and tumor tissue from wild-type and mutant mice for cell culture or histological analysis were carried out in compliance with the Emory University Institutional Animal Care and Use Committee guidelines. NeuroD2-SmoA1 mice were provided by Jim Olson (Fred Hutchinson Cancer Research Center), and bred in house. SmoA1 mice were crossed with Math1-GFP mice to produce SmoA1-GFP genetically engineered mice. The tumor bearing SmoA1 mice used in this study were males and females 4–6 months of age. The wild-type neonatal mice used to collect CGNPs were not discriminated based on sex.

Cerebellar Granule Neuron Precursor Culture

CGNP cultures were conducted as previously described (19). Cells were plated on poly-DL-ornithine (Sigma) pre-coated plates. Where indicated, Shh was used at a concentration of 3 $\mu\text{g}/\text{mL}$ and cyclopamine (R&D Systems) was used at 1 $\mu\text{g}/\text{mL}$. Cells were seeded in 10% FBS N2 media for two hours before being switched to serum-free N2 media. Where indicated, Apocynin, N-acetyl-L-cysteine (NAC), or Glutathione (GSH) was administered after 24 hours in serum-free media at the stated concentration for the given duration. Notably, due to NAC's short half-life, it was supplemented every 6 hours during treatment.

Protein Collecting and Immunoblotting

Tissue samples or cells were collected, washed once with 1x PBS, then resuspended in complete lysis buffer and whole cell lysates were generated as previously described (19). The Bradford assay and the Coomassie plus protein assay reagent (Thermo Scientific) were used to estimate protein concentrations. 20µg of each sample were separated by sodium dodecyl sulfate-polyacrylamide gel electrophoresis (SDS-PAGE) on 8 or 10% gels and transferred to activated Immobilon PVDF membranes (Millipore). Western blotting was carried out according to standard protocols. Primary antibodies used: anti-HIF1 α (Novus Biologicals), anti-Nox4 (Abcam), anti-Cleaved Caspase-3 (Cell Signaling), anti-cyclin D2 (Santa Cruz Biotechnology), anti-cyclin D1 (Abcam), anti-PHD2 (Cell Signaling), anti-PHD3 (Abcam), anti-Phospho-rpS6 (Cell Signaling), anti-HKII (Cell Signaling), anti-PKM2 (Cell Signaling), anti-Sox2 (Abcam) and anti- β -actin (Sigma). Horseradish peroxidase conjugated secondary antibodies used were anti-mouse and goat anti-rabbit. Western blots were developed using the ECL reagent (Thermo Scientific) and then exposing membranes to GE-Amersham chemiluminescence film for varying periods of time to achieve optimal saturation.

***Ex Vivo* Organotypic SmoA1 Tumor Slice Culture**

SmoA1-GFP tumors were embedded in 4% agarose and sliced on a sagittal plane into 300µm-thick slices with a vibratome (Leica VT1200S). Slices were placed on transwell inserts (1µm pore size; Falcon, Tewksbury MA) in Neurobasal (NB) Medium (Gibco) supplemented with B27 (Gibco), penicillin-streptomycin, N2 supplement (Gibco), L-Glutamine (Glutamax, Gibco) and sodium-pyruvate (Gibco). The slices were

cultured for 24 hours before administration of Apocynin, N-acetyl-L-cysteine (NAC), or Glutathione (GSH) at the stated concentration for the given duration. NAC was replenished every 6 hours. Tumor slices were collected at indicated time points for lysing and western blotting as stated above.

Immunofluorescence

Immunofluorescence was performed on SmoA1 tumor sections. SmoA1 Mice, upon showing symptoms of tumor burden, received whole-body perfusion of 4% PFA with the tumor and adjacent cerebellum processed and sectioned. Tumors were fixed overnight in 4% PFA followed by 24 hours in 30% sucrose/1xPBS, a cryoprotectant. Samples were frozen in O.C.T. compound (Tissue Tek, Sakura) and cut along a sagittal plane into 6-8 μ m-thick sections using a cryostat (Leica CM1860). 5% bovine serum albumin (BSA)/1xPBS+0.1% Triton blocking buffer was used. Immunofluorescence on sections was performed using standard methods. Antibodies used include: anti-HIF1 α (Abcam), anti-Nestin (Abcam), Anti-CD31 (Abcam), and donkey anti-mouse and rabbit IgG (Life technologies).

Reactive Oxygen Species Assay

CGNPs were cultured as stated above in six-well plates. At 48 hours, CGNPs were washed in warm 1x PBS and harvested by trypsinization (250 μ L of 0.05% trypsin). 10% FBS N2 media was added to stop trypsinization and cells were transferred to 1.5mL tubes where they were washed in warm 1x PBS, pelleted, and resuspended in warm 1x Hank's Balanced Salt Solution (HBSS) and transferred to black 1.5mL tubes where 2 μ L

of 10 μ M CM-H₂DCFDA solution were added to each. Samples were placed in a cell incubator [(37 °C), high relative humidity (95%), and controlled CO₂ level (5%)] in the dark for 45 min. CGNPs were resuspended by pipetting, and 200 μ L aliquots were added to a black 96-well plate. Fluorescence of DCF, the activated form of CM-H₂DCFDA when it comes in contact with ROS, was quantified on a Glomax plate reader.

Results

HIF1 α is Up-regulated in SmoA1 MB Tumors

HIF1 α transcriptional activity has been extensively studied with significant evidence indicating that its target gene expression leads to increased invasiveness, therapy-resistance, and overall poor prognosis. Although HIF1 α transactivation is associated with adverse patient outcomes, its role is not well understood in the context of cerebellar development and medulloblastoma formation.

Before proceeding with an investigation of mechanisms regulating HIF1 α stability we confirmed a significant increase in HIF1 α levels in Shh-driven MB using our NeuroD2-SmoA1 mouse model (see materials/methods). Tumors were resected upon onset of symptoms in mice, typically at 4-6 months of age. SmoA1-GFP mice (see materials/methods) that mimic Shh MB *in vivo* but with tumor cells expressing GFP, were used to reliably distinguish between MB tissue and the adjacent normal cerebellum. Whole cell lysates were generated and western blotting was performed according to standard methods. As expected, HIF1 α protein levels were significantly higher in medulloblastoma tissue compared to the non-GFP expressing normal cerebellum (MB and CB, respectively in Fig. 13). These results agreed with our preliminary studies (Fig. 5A; Fig. 12B) described earlier.

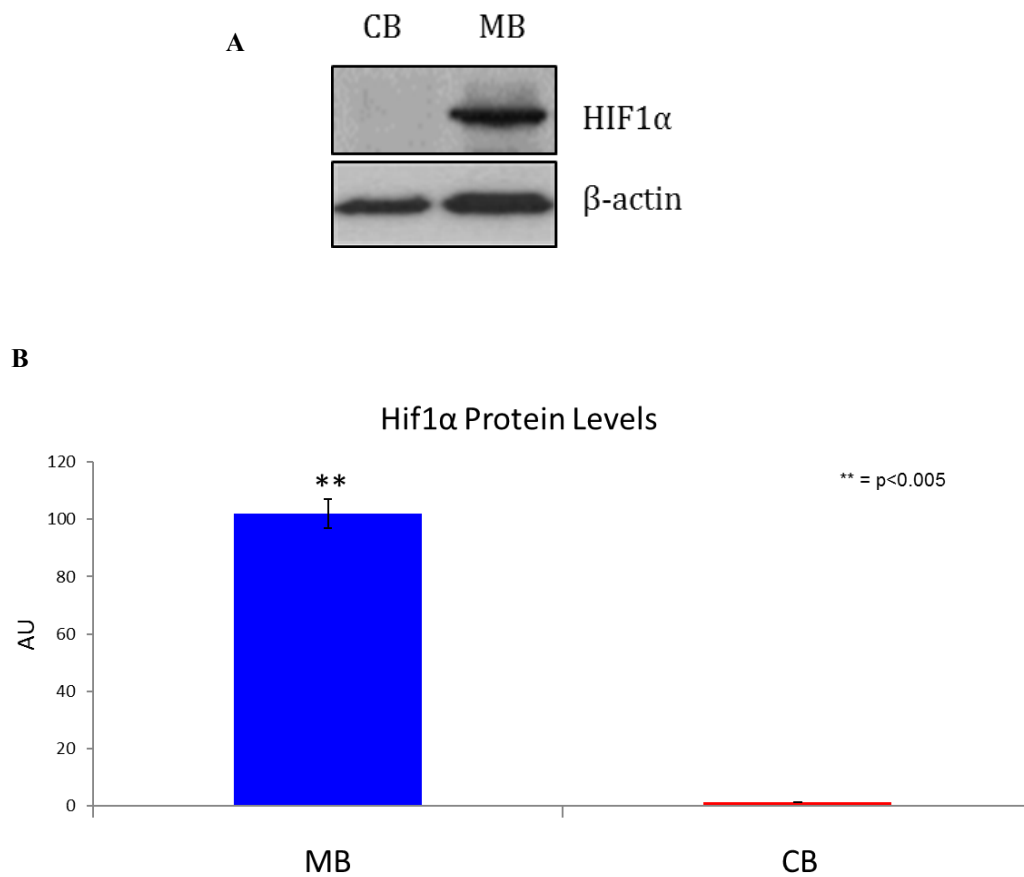


Figure 13. HIF1α Protein is up-regulated in SmoA1 MB: (A) Immunoblot analysis indicating an increase in HIF1α protein levels in SmoA1 tumor tissue compared to neighboring normal cerebellum. (B) Quantification of HIF1α levels using densitometry; Western blots were carried out using material from 3 separate mice; N=3, Student's t-test; **p<0.005.

HIF1 α Colocalizes with Stem Cell Markers in the MB Perivascular Niche

The tumor perivascular niche (PVN) is of particular interest when identifying novel therapeutic strategies against MB. The PVN is extremely intricate and is home to radiation-resistant tumor stem cells that have been shown to drive recurrence, which is lethal in MB patients. Given HIF1 α 's established role in promoting stem-like qualities in congruence with preliminary data (Fig. 6A), we performed immunofluorescence on fixed/frozen SmoA1 tumor sections to identify localization of HIF1 α within our MB model. We observed positive staining for HIF1 α in hypoxic areas of the tumor bulk (data not shown) as well as around the blood vessels (Fig. 14A). Nestin-positive neural stem-like cells localized around the vasculature as well in serial sections (Fig. 14B). Finally, co-staining for HIF1 α and Nestin added confirmation that they are both present in the PVN (Fig. 14C), an attractive therapeutic target.

These findings support previous work in the lab identifying HIF1 α stabilization in the oxygen-containing tumor PVN. Taken together, these observations backed our hypothesis that hypoxia-independent regulation of HIF1 α could be at play in the MB PVN, provoking further investigation of HIF1 α potentially playing a role in radiation-surviving stem cell maintenance.

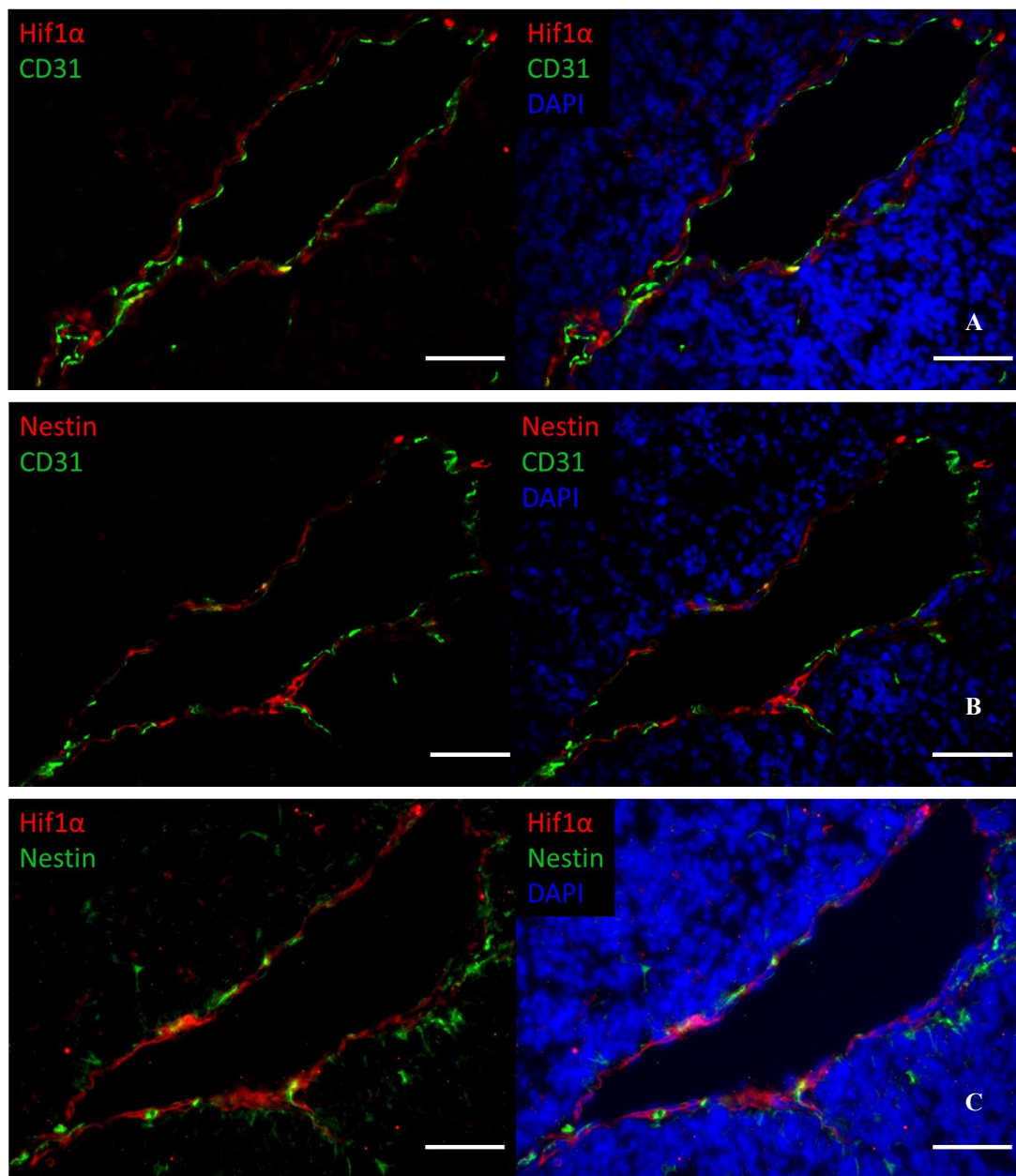


Figure 14. HIF1 α Colocalizes with Stem Cell Markers in the Medulloblastoma Perivascular Niche: (A) Immunofluorescence (I.F.) showing HIF1 α positive staining (red) around a tumor blood vessel indicated by CD31 staining (green). (B) I.F. showing neural stem cell marker Nestin positive cells (red) around a tumor blood vessel indicated by CD31 staining (green). (C) I.F. showing HIF1 α positive staining (red) within and surrounding Nestin-positive cells of the PVN (green). SmoA1 fixed/frozen tumor sections; N=1; Scale Bar = 50 μ m

HIF1 α Protein is Up-regulated in Shh-treated CGNPs

CGNPs are the putative cells of origin for the Shh subclass of medulloblastoma. Primary culture of these cells (see materials/methods) at P5 in the presence of exogenous Shh elegantly recapitulates the aberrant Shh signaling involved in MB initiation and progression. This *in vitro* system allows us to study Shh mitogenic and oncogenic signaling and how downstream components can contribute to CGNP transformation. Using this system we confirmed our preliminary findings (Fig. 7A; Fig. 7C) that Shh induces HIF1 α in CGNPs, in particular that HIF1 α levels are being regulated post-transcriptionally. To do so, CGNPs from neonatal mice were harvested and vehicle- or Shh-treated for 48hrs. Whole cell lysates were generated and western blotting was performed according to standard methods (see materials/methods). CGNPs that received Shh displayed higher levels of HIF1 α protein compared to vehicle-treated CGNPs (Fig. 15A). Notably, levels of PHD2/PHD3 increased as well, which agrees with HIF1 α 's known function in driving its own negative feedback loop. Cyclin D2 is used as a proliferation marker and confirms Shh pathway activation in CGNPs. We then proceeded to treat CGNPs with a combination of Shh and the mTOR inhibitor rapamycin, noting a decrease in HIF1 α over time (Fig. 15B). Reduced phosphorylation of ribosomal protein S6 (rpS6) serves as confirmation of mTOR inhibition. This finding is consistent with previous work implying that Shh-induced HIF1 α stabilization is a post-transcriptional process.

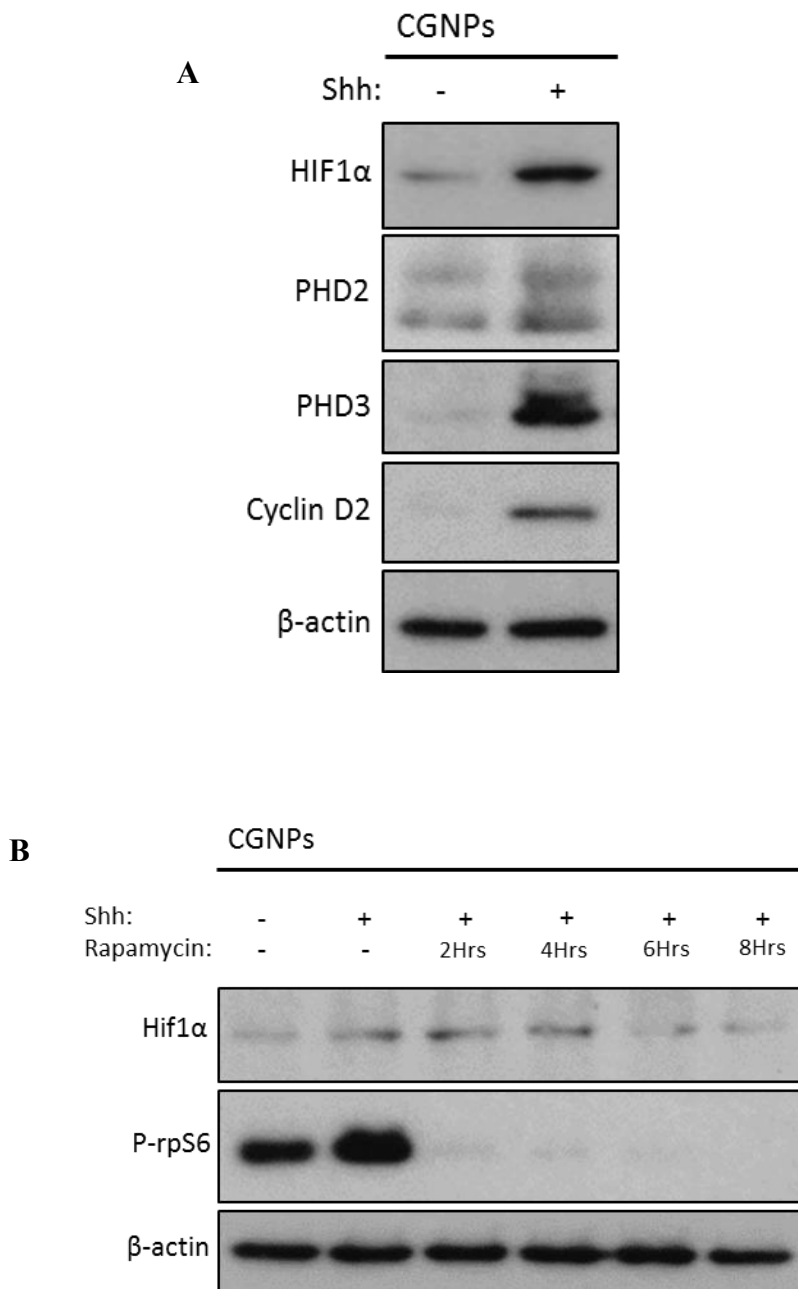


Figure 15. Hif1 α Protein is Up-regulated in Shh-treated CGNPs: (A) Immunoblot showing up-regulation of Hif1 α and Nox4 induced by Shh. PHD2/3 are also up in Shh-treated CGNPs, which are conventionally up-regulated by Hif1 α to mediate its own degradation. (B). Treating CGNPs with Shh followed by the mTOR inhibitor rapamycin reduced Hif1 α protein levels overtime. Lack of rpS6 phosphorylation confirms mTOR inhibition. N=1.

Shh Induces ROS Production in CGNPs

To test the hypothesis that ROS signaling is downstream of Shh, we first measured the concentration of ROS in CGNPs treated with exogenous Shh. We proceeded to thoroughly optimize a ROS assay using 5-(and 6-)Chloromethyl-2',7'-dichlorodihydro-fluorescein diacetate (CM-H₂DCFDA), which had mainly been used in cell lines. Therefore we developed a protocol for primary cell culture. CM-H₂DCFDA is a molecule that is hydrolyzed and rendered active upon entering the cell and it cannot freely diffuse from the cell. This compound fluoresces at 520nm when oxidized by cellular ROS. Its ability to stay within the cell avoids false signals from extracellular ROS. With a standard curve generated by adding known quantities of hydrogen peroxide to cells prior to CM-H₂DCFDA administration, we were able to measure changes in ROS concentration among CGNPs under different culture conditions.

Using this assay, we have consistently observed increased levels of ROS on the scale of several hundred nanomolar following Shh treatment and a reduction in ROS production to control levels with the addition of cyclopamine, a Smo-dependent Shh pathway inhibitor (Fig. 16). Combined with previous data, ROS induction resulting from Shh signaling follows the same pattern as HIF1 α protein levels, thus strengthening the claim that ROS could be involved in its stabilization. This assay is a very powerful tool moving forward with our ROS-mediated HIF1 α stabilization hypothesis.

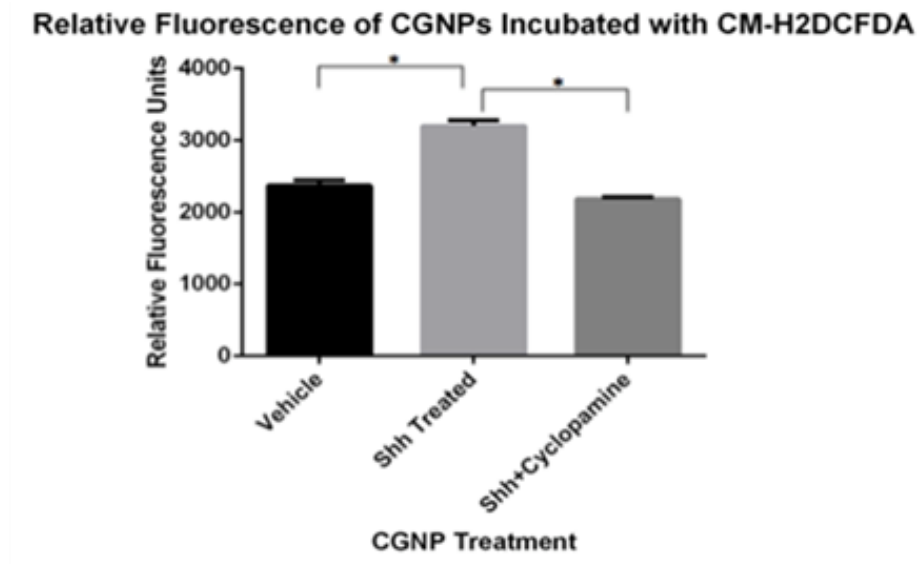


Figure 16. Shh Induces ROS Production in CGNPs: ROS assays were performed on CGNPs using CM-H₂DCFDA, a molecule that fluoresces after coming in contact with intracellular ROS. Shh treatment of CGNPs induces a significant increase in ROS levels compared to vehicle and Shh inhibition using cyclopamine. N=1. *p<0.05

Antioxidant-Mediated Sequestering of ROS Reduces HIF1 α Protein Stabilization in Shh-treated CGNPs and in SmoA1 Medulloblastomas Ex Vivo

With evidence linking Shh to higher levels of intracellular ROS production in CGNPs, we decided to scavenge these radicals using the very common antioxidant N-acetyl-L-cysteine (NAC) *in vitro* and ask if HIF1 α was destabilized. CGNPs from neonatal mice were cultured in the presence or absence of exogenous Shh (see materials/methods) in serum-free medium for 24 hours before NAC (10mM) was added and replenished every 6 hours for the indicated time points. All cells were collected, lysed, and analyzed via western blot. Shh treatment alone showed expected high levels of HIF1 α and Cyclin D1 protein, but levels of both diminished with NAC treatment over time (Fig. 17A). Furthermore, we applied this pharmacological method to our *ex vivo* MB slice culture system to gain more tumorigenically relevant insight. NAC was administered just as in CGNPs and doing so resulted in similar decreases in HIF1 α and Cyclin D1 protein by western blotting as well (Fig. 17B).

Additionally, we performed the same experiments using a different antioxidant Glutathione (GSH) at a concentration of 5mM. We observed a similar drop in HIF1 α and cyclin D1 in CGNPs treated with Shh and GSH (Fig. 18A). This trend was also seen in MB tumor slice culture as well (Fig, 18B). These data continue to support the involvement of ROS signaling in HIF1 α hypoxia-independent regulation.

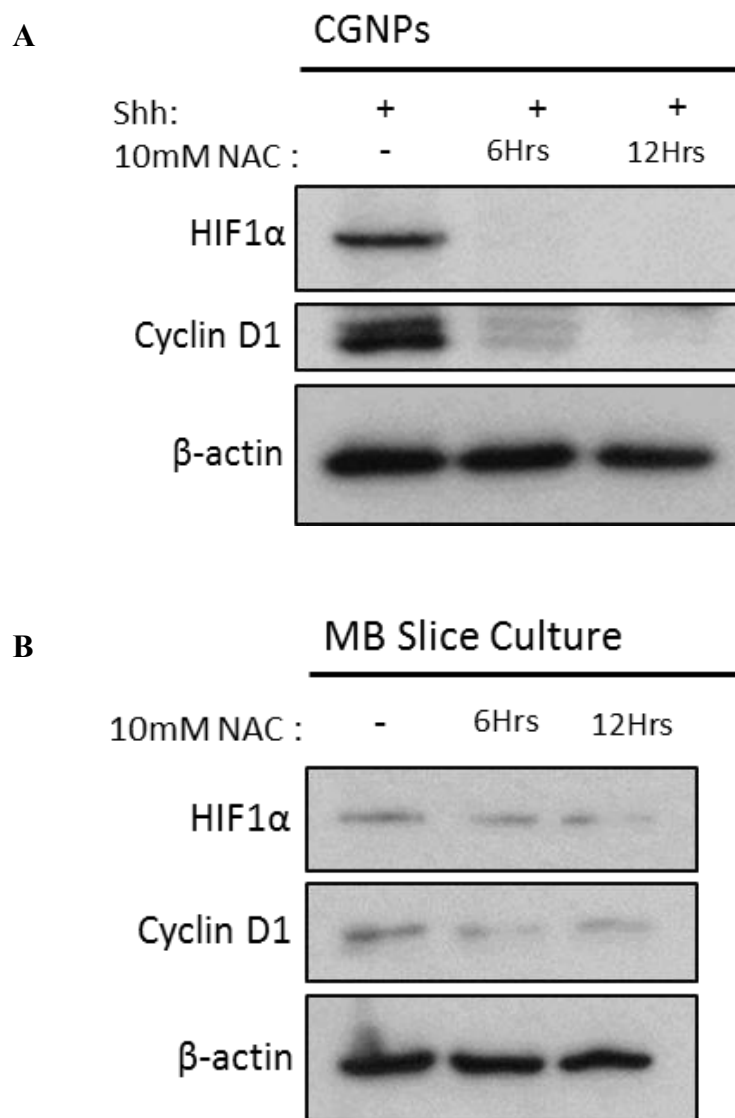


Figure 17. Immunoblot Analysis Following ROS Scavenging using NAC in Shh-Treated CGNPs and SmoA1 Medulloblastomas *Ex Vivo*: (A). CGNPs were treated with NAC (10mM) alongside Shh for 6 and 12 hours. NAC was supplemented every 6 hours. Note decreased HIF1 α levels after ROS depletion. (B). 300 μ m-thick SmoA1 tumor slices were cultured in NB-B27 medium and also treated with NAC (10mM) for 6 and 12 hours with drug replenishment every 6 hours as well. N=1.

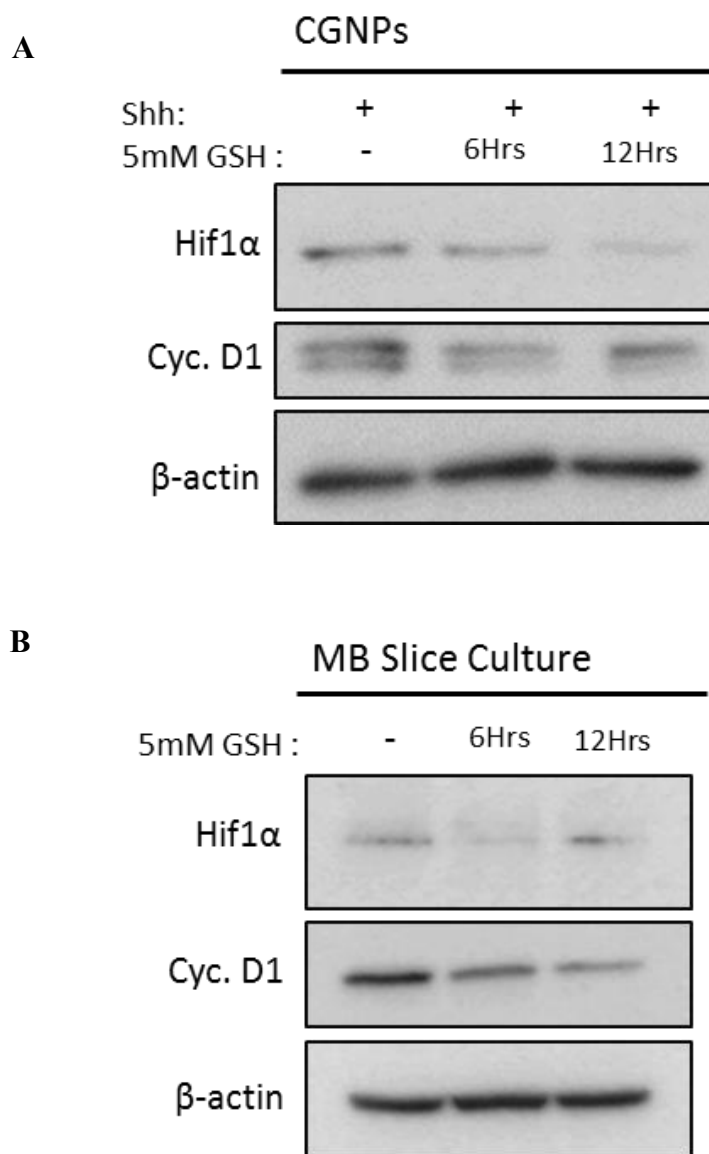


Figure 18. Immunoblot Analysis Following ROS Scavenging with GSH in Shh-Treated CGNPs and SmoA1 Medulloblastomas *Ex Vivo*: (A). CGNPs were treated with GSH (5mM) alongside Shh for 6 and 12 hours. GSH was supplemented every 6 hours. Note decreased HIF1 α levels after ROS depletion. (B). 300 μ m-thick SmoA1 tumor slices were cultured in NB-B27 medium and also treated with GSH (5mM) for 6 and 12 hours with drug replenishment every 6 hours as well. N=1.

NADPH Oxidase Inhibition Reduces HIF1 α Protein Stabilization in Shh-treated CGNPs and in SmoA1 Medulloblastomas Ex Vivo

Following treatment with NAC or GSH we wanted to test our hypothesis that Nox activity is involved in ROS production that stabilizes HIF1 α . CGNPs and MB slices were cultured in the same manner as with our NAC/GSH experiments (Fig. 18/19), but in this case the Nox inhibitor apocynin was added at indicated concentrations for 24 hours. Western blot analysis revealed similar results as with NAC/GSH in that HIF1 α levels decreased in CGNPs and tumor slices but this time in an apocynin dose-dependent manner. Additionally, PHD3 levels continued to correlate with HIF1 α levels, and Cyclin D2 signal decreased with apocynin treatment (Fig. 19A; Fig. 19B).

NADPH Oxidase 4 is Upregulated Downstream of Shh

In order to identify the Nox family protein generating ROS we decided to investigate Nox4 given our previous data and the current literature linking it to various cancers and HIF1 α stabilization. Using our SmoA1 mouse model, we observed a clear increase in Nox4 protein levels in the tumor compared to the neighboring normal cerebellar tissue (Fig. 20A). We then treated CGNPs with exogenous Shh and again observed elevated Nox4 levels (Fig. 20B). Although very preliminary, these results support Nox4 as potentially playing a role in ROS-dependent HIF1 α stabilization.

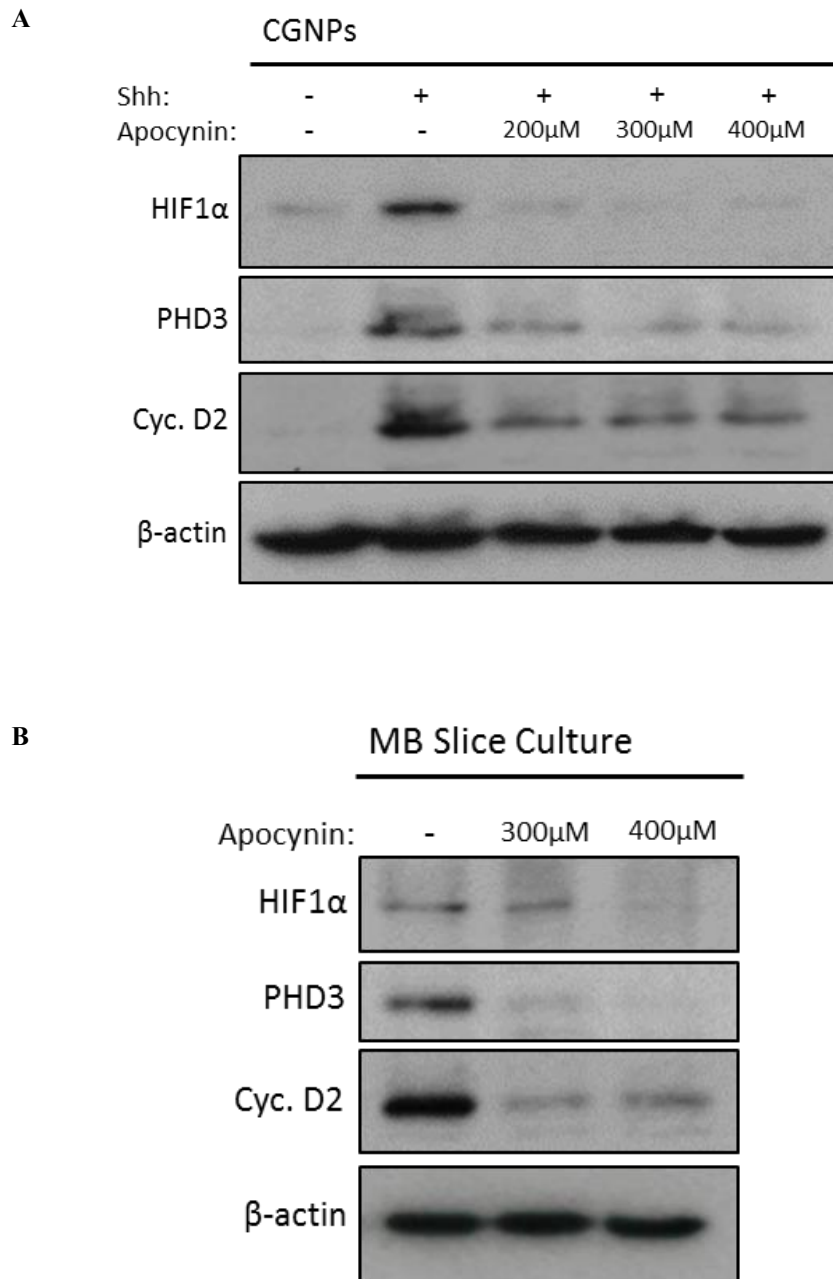


Figure 19. Immunoblot Analysis Following NADPH Oxidase Inhibition in Shh-Treated CGNPs and SmoA1 Medulloblastomas *Ex Vivo*: (A). CGNPs were treated with Apocynin at indicated concentrations combined with Shh for 24 hours. Note decreased HIF1 α levels after inhibiting NADPH Oxidase ROS production. (B). 300 μ m-thick SmoA1 tumor slices were cultured in NB-B27 medium and also treated with Apocynin for 24 hours. N=1.

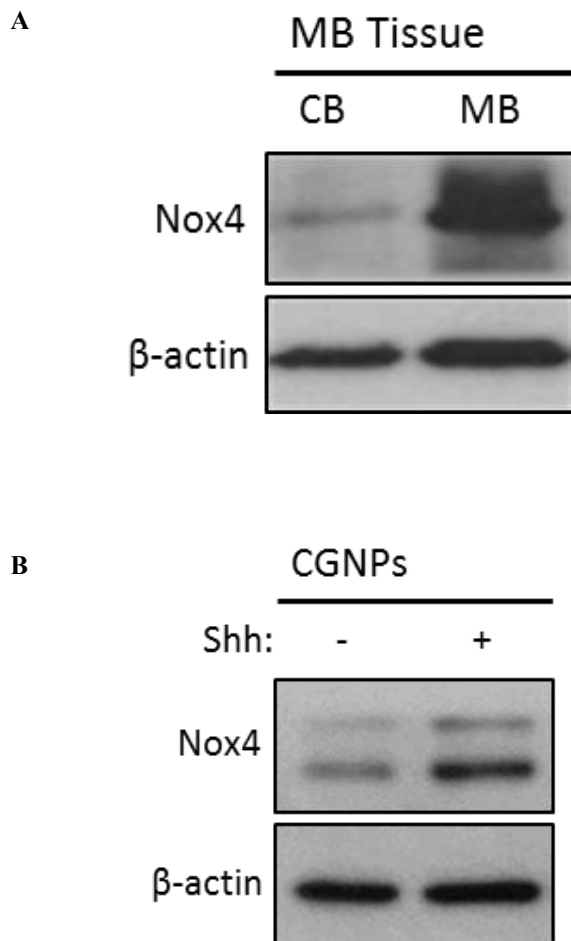


Figure 20. Nox4 Protein is Up-regulated in MB and Shh-treated CGNPs: (A) Immunoblot analysis indicating an increase in Nox4 protein levels in SmoA1 tumor tissue compared to neighboring normal cerebellum. (B) Immunoblot analysis showing up-regulation of Nox4 induced by Shh in CGNPs. N=1.

Discussion

Medulloblastoma comprises the most common CNS malignancy among children, with approximately 30% of these tumors belonging to the Sonic Hedgehog molecular subclass. Although the current standard of care leads to a relatively high “cure” rate (~70%), patients are left with a myriad of neurological and developmental deficits; this indicates a substantial need for development of novel molecular targeted therapies. Furthermore, medulloblastoma recurrence is lethal and is driven by radiation-resistant cancer stem cells residing in the tumor perivascular niche (PVN). The mechanisms by which these cells survive therapies remain largely unclear and further investigation is essential in working toward patient recurrence-free survival.

To reliably recapitulate spontaneous tumors arising from aberrant Shh signaling, we used a NeuroD2-SmoA1 mouse model. We also took advantage of an *in vitro* cerebellar granule neuron precursor (CGNP) primary culture system that allows us to closely study Shh mitogenic signaling and its downstream interactions/effectors. In this study, we examined the role of reactive oxygen species (ROS) signaling in the hypoxia-independent (non-canonical) stabilization and transactivation of HIF1 α in Shh-driven medulloblastoma. HIF1 α levels are rate-limiting in HIF-1 transcriptional activation. It has been widely studied and accepted as an essential player in various aspects of cancer progression including maintenance of stem-like qualities (47-53). These reports are consistent with our finding of HIF1 α within and surrounding nestin-positive stem-like cells in the medulloblastoma PVN (Fig. 14). Since these cells reside in the well-oxygenated area surrounding the vasculature, we were lead to investigate hypoxia-independent factors contributing to this HIF1 α stability. Accumulation of intracellular ROS has been shown to hinder the process by which HIF1 α is degraded, independent of

the oxygenation state (7, 75-83). These reports are consistent with our finding the HIF1 α is upregulated in medulloblastoma compared to the adjacent normal cerebellum in a post-transcriptional manner. Congruently, Shh pathway induction in CGNPs results in a significant increase in ROS levels along with marked HIF1 α protein stabilization. Follow-up experiments aimed at directly sequestering ROS used the antioxidants N-acetyl-L-cysteine (NAC) or Glutathione (GSH). Administering NAC or GSH to Shh-treated CGNPs and *ex vivo* tumor slices resulted in diminished HIF1 α levels.

The current literature supports the NADPH oxidase (Nox) family of proteins as being a significant regulator of intracellular ROS production in a multitude of cancers (1, 84-86, 95, 96) and their activity has been linked to HIF1 α stabilization (84, 85, 91-93). We considered these findings within the context of our hypothesis. Strikingly, we found that inhibiting Nox activity pharmacologically using apocynin decreased HIF1 α levels in Shh-treated CGNPs and *ex vivo* tumor slice culture. Taken together, our results and other studies indicate a potential role for Nox-generated ROS in hypoxia-independent HIF1 α transactivation. Preliminary findings and other studies suggest that Nox4, one of the 7 human Nox homologues, could be of particular interest within our paradigm (97-105). Furthermore, Nox4 is up-regulated in medulloblastoma compared to the neighboring normal cerebellum and elevated in Shh-treated CGNPs. Much work is necessary to establish a stronger correlation or even a causal role, but so far Nox4 induction has accompanied HIF1 α stabilization in our working models.

While promising, this study does present with a number of limitations. Our *in vitro* and *ex vivo* cultures are grown in a standard incubator with an approximate pO₂ of 21%, which results in hyperoxic conditions compared to physiological pO₂. Additionally,

the ROS assay used does not detect all forms of ROS, but it does detect the most common Nox-produced ROS types. Of course, reproducing these findings is necessary to build statistical strength and gain a clearer idea of what is happening within our system. These discrepancies as well as always-present tumor heterogeneity should be considered when interpreting the physiological relevance of these results.

Follow-up studies include performing the ROS assay after treatment of CGNPs and tumor slices with NAC, GSH, or apocynin to confirm that those drugs did in fact reduce ROS levels. Also, rescuing hydroxylation of HIF1 α in Shh-treated CGNPs and Tumor slices with FeCl₂ treatment would indicate ROS pushing ferrous iron toward the ferric state as in (91). In the future, we would like to assess whether the drop in HIF1 α in tumor slices following antioxidant or apocynin treatment occurs around the vasculature. This direction involves using the same tumor slice culture methods and then performing immunofluorescence analysis of HIF1 α around endothelial cells using the marker CD31. This experiment would give a better indication of ROS-mediated stabilization of HIF1 α in the elusive tumor perivascular niche. If this relationship is further elucidated, we would also like to explore the recently proposed cycling hypoxia theory as a means of Nox4-mediated ROS production near the vasculature which has been shown to drive brain tumor radiation resistance (101, 106). Spatial and temporal fluctuations in oxygen levels surrounding new and disorganized tumor vasculature lead to ROS generation, tumor-promoting inflammation, and angiogenesis (107, 108). The kinetics underlying this oxygen instability are not well known, but resulting oxidative stress has been linked to HIF1 α and its expression in the tumor PVN (109, 110). This theory is valuable as we work to understand the relationship between Nox4 and HIF1 α . Lentiviral knockdown of

Nox4 will also be pursued to establish a relationship between Nox4 activity and HIF1 α stabilization.

Overall, this work supports intracellular ROS playing a role in hypoxia-independent HIF1 α stabilization and transactivation in Shh-driven medulloblastoma. This could lead to a better understanding of the mechanisms underlying HIF1 α activity in the tumor perivascular niche, which has been shown to contribute to stemness, radiation resistance, and lethal recurrence. Learning how tumor stem cells are able to resist radiation is essential in working toward disease-free survival, and we believe our proposed Nox4—ROS—HIF1 α axis (Fig. 21) could provide valuable clues in understanding this process.

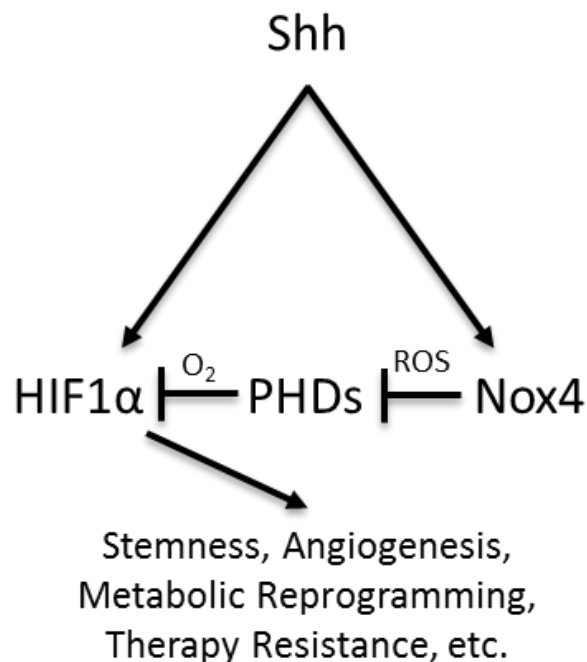


Figure 21. Proposed Nox4—ROS—HIF1 α Model

References

1. Brandes RP, Weissmann N, Schroder K. Nox family NADPH oxidases: Molecular mechanisms of activation. *Free radical biology & medicine*. 2014;76:208-26. Epub 2014/08/27. doi: 10.1016/j.freeradbiomed.2014.07.046. PubMed PMID: 25157786.
2. Northcott PA, Dubuc AM, Pfister S, Taylor MD. Molecular subgroups of medulloblastoma. *Expert Rev Neurother*. 2012;12(7):871-84. doi: 10.1586/ern.12.66. PubMed PMID: 22853794; PMCID: PMC4334443.
3. Mimura I, Nangaku M. The suffocating kidney: tubulointerstitial hypoxia in end-stage renal disease. *Nature reviews Nephrology*. 2010;6(11):667-78. Epub 2010/09/30. doi: 10.1038/nrneph.2010.124. PubMed PMID: 20877304.
4. Knoepfler PS, Kenney AM. Neural precursor cycling at sonic speed: N-Myc pedals, GSK-3 brakes. *Cell cycle (Georgetown, Tex)*. 2006;5(1):47-52. Epub 2005/12/03. doi: 10.4161/cc.5.1.2292. PubMed PMID: 16322694.
5. Liou GY, Storz P. Reactive oxygen species in cancer. *Free radical research*. 2010;44(5):479-96. Epub 2010/04/08. doi: 10.3109/10715761003667554. PubMed PMID: 20370557; PMCID: PMC3880197.
6. Keith B, Johnson RS, Simon MC. HIF1alpha and HIF2alpha: sibling rivalry in hypoxic tumour growth and progression. *Nature reviews Cancer*. 2011;12(1):9-22. Epub 2011/12/16. doi: 10.1038/nrc3183. PubMed PMID: 22169972; PMCID: PMC3401912.
7. Taylor CT. Mitochondria and cellular oxygen sensing in the HIF pathway. *Biochem J*. 2008;409(1):19-26. doi: 10.1042/BJ20071249. PubMed PMID: 18062771.
8. Mainwaring LA, Kenney AM. Divergent functions for eIF4E and S6 kinase by sonic hedgehog mitogenic signaling in the developing cerebellum. *Oncogene*. 2011;30(15):1784-97. Epub 2011/02/23. doi: 10.1038/onc.2010.564. PubMed PMID: 21339731; PMCID: PMC3583293.
9. Becker LE, Hinton D. Primitive neuroectodermal tumors of the central nervous system. *Hum Pathol*. 1983;14(6):538-50. PubMed PMID: 6303940.
10. Kosnik EJ, Boesel CP, Bay J, Sayers MP. Primitive neuroectodermal tumors of the central nervous system in children. *J Neurosurg*. 1978;48(5):741-6. doi: 10.3171/jns.1978.48.5.0741. PubMed PMID: 641553.
11. Packer RJ, Cogen P, Vezina G, Rorke LB. Medulloblastoma: clinical and biologic aspects. *Neuro Oncol*. 1999;1(3):232-50. PubMed PMID: 11550316; PMCID: PMC1920747.
12. Zagzag D, Miller DC, Knopp E, Farmer JP, Lee M, Biring S, Pellicer A, Epstein FJ, Allen JC. Primitive neuroectodermal tumors of the brainstem: investigation of seven cases. *Pediatrics*. 2000;106(5):1045-53. PubMed PMID: 11061774.
13. Millard NE, De Braganca KC. Medulloblastoma. *Journal of child neurology*. 2016;31(12):1341-53. Epub 2015/09/04. doi: 10.1177/0883073815600866. PubMed PMID: 26336203; PMCID: Pmc4995146.

14. Northcott PA, Korshunov A, Witt H, Hielscher T, Eberhart CG, Mack S, Bouffet E, Clifford SC, Hawkins CE, French P, Rutka JT, Pfister S, Taylor MD. Medulloblastoma comprises four distinct molecular variants. *J Clin Oncol*. 2011;29(11):1408-14. doi: 10.1200/JCO.2009.27.4324. PubMed PMID: 20823417; PMCID: PMC4874239.
15. Leto K, Arancillo M, Becker EB, Buffo A, Chiang C, Ding B, Dobyns WB, Dusart I, Haldipur P, Hatten ME, Hoshino M, Joyner AL, Kano M, Kilpatrick DL, Koibuchi N, Marino S, Martinez S, Millen KJ, Millner TO, Miyata T, Parmigiani E, Schilling K, Sekerkova G, Sillitoe RV, Sotelo C, Uesaka N, Wefers A, Wingate RJ, Hawkes R. Consensus Paper: Cerebellar Development. *Cerebellum* (London, England). 2016;15(6):789-828. Epub 2015/10/07. doi: 10.1007/s12311-015-0724-2. PubMed PMID: 26439486; PMCID: PMC4846577.
16. Eberhart CG. Even cancers want commitment: lineage identity and medulloblastoma formation. *Cancer cell*. 2008;14(2):105-7. Epub 2008/08/12. doi: 10.1016/j.ccr.2008.07.011. PubMed PMID: 18691544; PMCID: PMC4512647.
17. Hatten ME, Roussel MF. Development and cancer of the cerebellum. *Trends in neurosciences*. 2011;34(3):134-42. Epub 2011/02/15. doi: 10.1016/j.tins.2011.01.002. PubMed PMID: 21315459; PMCID: PMC3051031.
18. Behesti H, Marino S. Cerebellar granule cells: insights into proliferation, differentiation, and role in medulloblastoma pathogenesis. *The international journal of biochemistry & cell biology*. 2009;41(3):435-45. Epub 2008/08/30. doi: 10.1016/j.biocel.2008.06.017. PubMed PMID: 18755286.
19. Kenney AM, Rowitch DH. Sonic hedgehog promotes G(1) cyclin expression and sustained cell cycle progression in mammalian neuronal precursors. *Molecular and cellular biology*. 2000;20(23):9055-67. Epub 2000/11/14. PubMed PMID: 11074003; PMCID: Pmc86558.
20. Wechsler-Reya RJ, Scott MP. Control of neuronal precursor proliferation in the cerebellum by Sonic Hedgehog. *Neuron*. 1999;22(1):103-14. Epub 1999/02/23. PubMed PMID: 10027293.
21. Dahmane N, Ruiz i Altaba A. Sonic hedgehog regulates the growth and patterning of the cerebellum. *Development* (Cambridge, England). 1999;126(14):3089-100. Epub 1999/06/22. PubMed PMID: 10375501.
22. Wallace VA. Purkinje-cell-derived Sonic hedgehog regulates granule neuron precursor cell proliferation in the developing mouse cerebellum. *Current biology : CB*. 1999;9(8):445-8. Epub 1999/05/05. PubMed PMID: 10226030.
23. Guldal CG, Ahmad A, Korshunov A, Squatrito M, Awan A, Mainwaring LA, Bhatia B, Parathath SR, Nahle Z, Pfister S, Kenney AM. An essential role for p38 MAPK in cerebellar granule neuron precursor proliferation. *Acta neuropathologica*. 2012;123(4):573-86. Epub 2012/02/04. doi: 10.1007/s00401-012-0946-z. PubMed PMID: 22302101; PMCID: PMC3775951.
24. Kenney AM, Widlund HR, Rowitch DH. Hedgehog and PI-3 kinase signaling converge on Nmyc1 to promote cell cycle progression in cerebellar neuronal precursors.

Development (Cambridge, England). 2004;131(1):217-28. doi: 10.1242/dev.00891. PubMed PMID: 14660435.

25. Hahn H, Wojnowski L, Specht K, Kappler R, Calzada-Wack J, Potter D, Zimmer A, Muller U, Samson E, Quintanilla-Martinez L. Patched target Igf2 is indispensable for the formation of medulloblastoma and rhabdomyosarcoma. *J Biol Chem*. 2000;275(37):28341-4. PubMed PMID: 10884376.
26. Hartmann W, Koch A, Brune H, Waha A, Schuller U, Dani I, Denkhaus D, Langmann W, Bode U, Wiestler OD, Schilling K, Pietsch T. Insulin-like growth factor II is involved in the proliferation control of medulloblastoma and its cerebellar precursor cells. *Am J Pathol*. 2005;166(4):1153-62. PubMed PMID: 15793295.
27. Parathath SR, Mainwaring LA, Fernandez LA, Campbell DO, Kenney AM. Insulin receptor substrate 1 is an effector of sonic hedgehog mitogenic signaling in cerebellar neural precursors. *Development (Cambridge, England)*. 2008;135(19):3291-300. doi: 10.1242/dev.022871. PubMed PMID: 18755774; PMCID: PMC2673703.
28. Berman DM, Karhadkar SS, Hallahan AR, Pritchard JI, Eberhart CG, Watkins DN, Chen JK, Cooper MK, Taipale J, Olson JM, Beachy PA. Medulloblastoma growth inhibition by hedgehog pathway blockade. *Science (New York, NY)*. 2002;297(5586):1559-61. Epub 2002/08/31. doi: 10.1126/science.1073733. PubMed PMID: 12202832.
29. Hatton BA, Villavicencio EH, Tsuchiya KD, Pritchard JI, Ditzler S, Pullar B, Hansen S, Knoblaugh SE, Lee D, Eberhart CG, Hallahan AR, Olson JM. The Smo/Smo model: hedgehog-induced medulloblastoma with 90% incidence and leptomeningeal spread. *Cancer research*. 2008;68(6):1768-76. Epub 2008/03/15. doi: 10.1158/0008-5472.can-07-5092. PubMed PMID: 18339857.
30. Bhatia B, Northcott PA, Hambardzumyan D, Govindarajan B, Brat DJ, Arbiser JL, Holland EC, Taylor MD, Kenney AM. Tuberous sclerosis complex suppression in cerebellar development and medulloblastoma: separate regulation of mammalian target of rapamycin activity and p27 Kip1 localization. *Cancer research*. 2009;69(18):7224-34. Epub 2009/09/10. doi: 10.1158/0008-5472.can-09-1299. PubMed PMID: 19738049; PMCID: PMC2745891.
31. Dimitrova V, Arcaro A. Targeting the PI3K/AKT/mTOR signaling pathway in medulloblastoma. *Current molecular medicine*. 2015;15(1):82-93. Epub 2015/01/21. PubMed PMID: 25601471.
32. Eckerdt F, Goldman S, Plataniias LC. New insights into malignant cell survival mechanisms in medulloblastoma. *Cancer cell & microenvironment*. 2014;1(6). Epub 2014/01/01. doi: 10.14800/ccm.374. PubMed PMID: 26097864; PMCID: PMC4470493.
33. Mohan AL, Friedman MD, Ormond DR, Tobias M, Murali R, Jhanwar-Uniyal M. PI3K/mTOR signaling pathways in medulloblastoma. *Anticancer research*. 2012;32(8):3141-6. Epub 2012/07/31. PubMed PMID: 22843885.
34. Abel TW, Baker SJ, Fraser MM, Tihan T, Nelson JS, Yachnis AT, Bouffard JP, Mena H, Burger PC, Eberhart CG. Lhermitte-Duclos disease: a report of 31 cases with immunohistochemical analysis of the PTEN/AKT/mTOR pathway. *Journal of*

neuropathology and experimental neurology. 2005;64(4):341-9. Epub 2005/04/20. PubMed PMID: 15835270.

35. Crino PB. mTOR: A pathogenic signaling pathway in developmental brain malformations. *Trends in molecular medicine*. 2011;17(12):734-42. Epub 2011/09/06. doi: 10.1016/j.molmed.2011.07.008. PubMed PMID: 21890410.
36. Garza-Lombo C, Gonsebatt ME. Mammalian Target of Rapamycin: Its Role in Early Neural Development and in Adult and Aged Brain Function. *Frontiers in cellular neuroscience*. 2016;10:157. Epub 2016/07/06. doi: 10.3389/fncel.2016.00157. PubMed PMID: 27378854; PMCID: PMC4910040.
37. Sandsmark DK, Pelletier C, Weber JD, Gutmann DH. Mammalian target of rapamycin: master regulator of cell growth in the nervous system. *Histology and histopathology*. 2007;22(8):895-903. Epub 2007/05/16. doi: 10.14670/hh-22.895. PubMed PMID: 17503347.
38. Hartley D, Cooper GM. Role of mTOR in the degradation of IRS-1: regulation of PP2A activity. *Journal of cellular biochemistry*. 2002;85(2):304-14. Epub 2002/04/12. PubMed PMID: 11948686.
39. Bhatia B, Nahle Z, Kenney AM. Double trouble: when sonic hedgehog signaling meets TSC inactivation. *Cell cycle (Georgetown, Tex)*. 2010;9(3):456-9. Epub 2010/01/19. doi: 10.4161/cc.9.3.10532. PubMed PMID: 20081363.
40. Pocza T, Sebestyén A, Turanyi E, Krenacs T, Mark A, Sticz TB, Jakab Z, Hauser P. mTOR pathway as a potential target in a subset of human medulloblastoma. *Pathology oncology research : POR*. 2014;20(4):893-900. Epub 2014/04/17. doi: 10.1007/s12253-014-9771-0. PubMed PMID: 24737380.
41. Bhatia B, Hsieh M, Kenney AM, Nahle Z. Mitogenic Sonic hedgehog signaling drives E2F1-dependent lipogenesis in progenitor cells and medulloblastoma. *Oncogene*. 2011;30(4):410-22. Epub 2010/10/05. doi: 10.1038/onc.2010.454. PubMed PMID: 20890301; PMCID: Pmc3072890.
42. Bhatia B, Potts CR, Guldal C, Choi S, Korshunov A, Pfister S, Kenney AM, Nahle ZA. Hedgehog-mediated regulation of PPARgamma controls metabolic patterns in neural precursors and Shh-driven medulloblastoma. *Acta neuropathologica*. 2012;123(4):587-600. Epub 2012/03/13. doi: 10.1007/s00401-012-0968-6. PubMed PMID: 22407012; PMCID: Pmc3306783.
43. Gogvadze V, Orrenius S, Zhivotovsky B. Mitochondria in cancer cells: what is so special about them? *Trends in cell biology*. 2008;18(4):165-73. Epub 2008/02/26. doi: 10.1016/j.tcb.2008.01.006. PubMed PMID: 18296052.
44. Pouyssegur J, Dayan F, Mazure NM. Hypoxia signalling in cancer and approaches to enforce tumour regression. *Nature*. 2006;441(7092):437-43. Epub 2006/05/26. doi: 10.1038/nature04871. PubMed PMID: 16724055.
45. Wang GL, Jiang BH, Rue EA, Semenza GL. Hypoxia-inducible factor 1 is a basic-helix-loop-helix-PAS heterodimer regulated by cellular O₂ tension. *Proc Natl Acad Sci U S A*. 1995;92(12):5510-4. Epub 1995/06/06. PubMed PMID: 7539918; PMCID: PMC41725.

46. Semenza GL. Defining the role of hypoxia-inducible factor 1 in cancer biology and therapeutics. *Oncogene*. 2010;29(5):625-34. doi: 10.1038/onc.2009.441. PubMed PMID: 19946328; PMCID: PMC2969168.
47. Ajdukovic J. HIF-1--a big chapter in the cancer tale. *Experimental oncology*. 2016;38(1):9-12. Epub 2016/04/01. PubMed PMID: 27031712.
48. Mimeault M, Batra SK. Hypoxia-inducing factors as master regulators of stemness properties and altered metabolism of cancer- and metastasis-initiating cells. *Journal of cellular and molecular medicine*. 2013;17(1):30-54. Epub 2013/01/11. doi: 10.1111/jcmm.12004. PubMed PMID: 23301832; PMCID: PMC3560853.
49. Sadri N, Zhang PJ. Hypoxia-inducible factors: mediators of cancer progression; prognostic and therapeutic targets in soft tissue sarcomas. *Cancers*. 2013;5(2):320-33. Epub 2013/11/13. doi: 10.3390/cancers5020320. PubMed PMID: 24216979; PMCID: PMC3730324.
50. Semenza GL. HIF-1: upstream and downstream of cancer metabolism. *Current opinion in genetics & development*. 2010;20(1):51-6. Epub 2009/11/28. doi: 10.1016/j.gde.2009.10.009. PubMed PMID: 19942427; PMCID: PMC2822127.
51. Semenza GL. Hypoxia-inducible factor 1: regulator of mitochondrial metabolism and mediator of ischemic preconditioning. *Biochimica et biophysica acta*. 2011;1813(7):1263-8. Epub 2010/08/25. doi: 10.1016/j.bbamcr.2010.08.006. PubMed PMID: 20732359; PMCID: PMC3010308.
52. Semenza GL. Targeting hypoxia-inducible factor 1 to stimulate tissue vascularization. *Journal of investigative medicine : the official publication of the American Federation for Clinical Research*. 2016;64(2):361-3. Epub 2015/05/09. doi: 10.1097/jim.0000000000000206. PubMed PMID: 25955799; PMCID: PMC4636970.
53. Semenza GL. Vascular responses to hypoxia and ischemia. *Arteriosclerosis, thrombosis, and vascular biology*. 2010;30(4):648-52. Epub 2009/09/05. doi: 10.1161/atvbaha.108.181644. PubMed PMID: 19729615; PMCID: PMC2841694.
54. Burroughs SK, Kaluz S, Wang D, Wang K, Van Meir EG, Wang B. Hypoxia inducible factor pathway inhibitors as anticancer therapeutics. *Future Med Chem*. 2013;5(5):553-72. doi: 10.4155/fmc.13.17. PubMed PMID: 23573973; PMCID: PMC3871878.
55. Semenza GL. Targeting HIF-1 for cancer therapy. *Nature reviews Cancer*. 2003;3(10):721-32. Epub 2003/09/18. doi: 10.1038/nrc1187. PubMed PMID: 13130303.
56. Hambarzumyan D, Becher OJ, Holland EC. Cancer stem cells and survival pathways. *Cell cycle (Georgetown, Tex)*. 2008;7(10):1371-8. Epub 2008/04/19. PubMed PMID: 18421251.
57. Hambarzumyan D, Becher OJ, Rosenblum MK, Pandolfi PP, Manova-Todorova K, Holland EC. PI3K pathway regulates survival of cancer stem cells residing in the perivascular niche following radiation in medulloblastoma in vivo. *Genes & development*. 2008;22(4):436-48. Epub 2008/02/19. doi: 10.1101/gad.1627008. PubMed PMID: 18281460; PMCID: PMC2238666.

58. Hambardzumyan D, Squatrito M, Holland EC. Radiation resistance and stem-like cells in brain tumors. *Cancer cell*. 2006;10(6):454-6. Epub 2006/12/13. doi: 10.1016/j.ccr.2006.11.008. PubMed PMID: 17157785.
59. Harada H, Inoue M, Itasaka S, Hirota K, Morinibu A, Shinomiya K, Zeng L, Ou G, Zhu Y, Yoshimura M, McKenna WG, Muschel RJ, Hiraoka M. Cancer cells that survive radiation therapy acquire HIF-1 activity and translocate towards tumour blood vessels. *Nature communications*. 2012;3:783. doi: 10.1038/ncomms1786. PubMed PMID: 22510688; PMCID: PMC3337987.
60. Meijer TW, Kaanders JH, Span PN, Bussink J. Targeting hypoxia, HIF-1, and tumor glucose metabolism to improve radiotherapy efficacy. *Clinical cancer research : an official journal of the American Association for Cancer Research*. 2012;18(20):5585-94. Epub 2012/10/17. doi: 10.1158/1078-0432.ccr-12-0858. PubMed PMID: 23071360.
61. Moeller BJ, Cao Y, Li CY, Dewhirst MW. Radiation activates HIF-1 to regulate vascular radiosensitivity in tumors: role of reoxygenation, free radicals, and stress granules. *Cancer cell*. 2004;5(5):429-41. PubMed PMID: 15144951.
62. Hu CJ, Iyer S, Sataur A, Covello KL, Chodosh LA, Simon MC. Differential regulation of the transcriptional activities of hypoxia-inducible factor 1 alpha (HIF-1alpha) and HIF-2alpha in stem cells. *Molecular and cellular biology*. 2006;26(9):3514-26. Epub 2006/04/14. doi: 10.1128/mcb.26.9.3514-3526.2006. PubMed PMID: 16611993; PMCID: PMC1447431.
63. Majmundar AJ, Wong WJ, Simon MC. Hypoxia-inducible factors and the response to hypoxic stress. *Molecular cell*. 2010;40(2):294-309. Epub 2010/10/23. doi: 10.1016/j.molcel.2010.09.022. PubMed PMID: 20965423; PMCID: PMC3143508.
64. Abraham RT. mTOR as a positive regulator of tumor cell responses to hypoxia. *Current topics in microbiology and immunology*. 2004;279:299-319. Epub 2003/10/17. PubMed PMID: 14560965.
65. Hudson CC, Liu M, Chiang GG, Otterness DM, Loomis DC, Kaper F, Giaccia AJ, Abraham RT. Regulation of hypoxia-inducible factor 1alpha expression and function by the mammalian target of rapamycin. *Molecular and cellular biology*. 2002;22(20):7004-14. Epub 2002/09/21. PubMed PMID: 12242281; PMCID: PMC139825.
66. Mi C, Ma J, Wang KS, Zuo HX, Wang Z, Li MY, Piao LX, Xu GH, Li X, Quan ZS, Jin X. Imperatorin suppresses proliferation and angiogenesis of human colon cancer cell by targeting HIF-1alpha via the mTOR/p70S6K/4E-BP1 and MAPK pathways. *Journal of ethnopharmacology*. 2017. Epub 2017/03/28. doi: 10.1016/j.jep.2017.03.033. PubMed PMID: 28341244.
67. White NM, Masui O, Newsted D, Scorilas A, Romaschin AD, Bjarnason GA, Siu KW, Yousef GM. Galectin-1 has potential prognostic significance and is implicated in clear cell renal cell carcinoma progression through the HIF/mTOR signaling axis. *British journal of cancer*. 2017;116(6):e3. Epub 2017/01/13. doi: 10.1038/bjc.2016.441. PubMed PMID: 28081542.

68. Gupta A, Rosenberger SF, Bowden GT. Increased ROS levels contribute to elevated transcription factor and MAP kinase activities in malignantly progressed mouse keratinocyte cell lines. *Carcinogenesis*. 1999;20(11):2063-73. Epub 1999/11/05. PubMed PMID: 10545407.
69. Li Q, Fu GB, Zheng JT, He J, Niu XB, Chen QD, Yin Y, Qian X, Xu Q, Wang M, Sun AF, Shu Y, Rui H, Liu LZ, Jiang BH. NADPH oxidase subunit p22(phox)-mediated reactive oxygen species contribute to angiogenesis and tumor growth through AKT and ERK1/2 signaling pathways in prostate cancer. *Biochimica et biophysica acta*. 2013;1833(12):3375-85. Epub 2013/10/12. doi: 10.1016/j.bbamcr.2013.09.018. PubMed PMID: 24113386.
70. Storz P. Reactive oxygen species in tumor progression. *Frontiers in bioscience : a journal and virtual library*. 2005;10:1881-96. Epub 2005/03/17. PubMed PMID: 15769673.
71. Szatrowski TP, Nathan CF. Production of large amounts of hydrogen peroxide by human tumor cells. *Cancer research*. 1991;51(3):794-8. Epub 1991/02/01. PubMed PMID: 1846317.
72. Kim YW, Byzova TV. Oxidative stress in angiogenesis and vascular disease. *Blood*. 2014;123(5):625-31. Epub 2013/12/05. doi: 10.1182/blood-2013-09-512749. PubMed PMID: 24300855; PMCID: PMC3907751.
73. Chaudhari P, Ye Z, Jang YY. Roles of reactive oxygen species in the fate of stem cells. *Antioxidants & redox signaling*. 2014;20(12):1881-90. Epub 2012/10/17. doi: 10.1089/ars.2012.4963. PubMed PMID: 23066813; PMCID: PMC3967382.
74. Hao Y, Cheng D, Ma Y, Zhou W, Wang Y. The relationship between oxygen concentration, reactive oxygen species and the biological characteristics of human bone marrow hematopoietic stem cells. *Transplantation proceedings*. 2011;43(7):2755-61. Epub 2011/09/14. doi: 10.1016/j.transproceed.2011.06.026. PubMed PMID: 21911158.
75. Klumpen E, Hoffschroer N, Zeis B, Gigengack U, Dohmen E, Paul RJ. Reactive oxygen species (ROS) and the heat stress response of *Daphnia pulex*: ROS-mediated activation of hypoxia-inducible factor 1 (HIF-1) and heat shock factor 1 (HSF-1) and the clustered expression of stress genes. *Biology of the cell*. 2017;109(1):39-64. doi: 10.1111/boc.201600017. PubMed PMID: 27515976.
76. Lim S, Liu H, Madeira da Silva L, Arora R, Liu Z, Phillips JB, Schmitt DC, Vu T, McClellan S, Lin Y, Lin W, Piazza GA, Fodstad O, Tan M. Immunoregulatory Protein B7-H3 Reprograms Glucose Metabolism in Cancer Cells by ROS-Mediated Stabilization of HIF1alpha. *Cancer research*. 2016;76(8):2231-42. doi: 10.1158/0008-5472.CAN-15-1538. PubMed PMID: 27197253; PMCID: PMC4874665.
77. Sarkar R, Mukherjee S, Biswas J, Roy M. Phenethyl isothiocyanate, by virtue of its antioxidant activity, inhibits invasiveness and metastatic potential of breast cancer cells: HIF-1alpha as a putative target. *Free radical research*. 2016;50(1):84-100. doi: 10.3109/10715762.2015.1108520. PubMed PMID: 26480821.
78. Seo S, Seo K, Ki SH, Shin SM. Isorhamnetin Inhibits Reactive Oxygen Species-Dependent Hypoxia Inducible Factor (HIF)-1alpha Accumulation. *Biological &*

- pharmaceutical bulletin. 2016;39(11):1830-8. Epub 2016/11/03. doi: 10.1248/bpb.b16-00414. PubMed PMID: 27803454.
79. Shatrov VA, Sumbayev VV, Zhou J, Brune B. Oxidized low-density lipoprotein (oxLDL) triggers hypoxia-inducible factor-1alpha (HIF-1alpha) accumulation via redox-dependent mechanisms. *Blood*. 2003;101(12):4847-9. Epub 2003/02/15. doi: 10.1182/blood-2002-09-2711. PubMed PMID: 12586627.
80. Shida M, Kitajima Y, Nakamura J, Yanagihara K, Baba K, Wakiyama K, Noshiro H. Impaired mitophagy activates mtROS/HIF-1alpha interplay and increases cancer aggressiveness in gastric cancer cells under hypoxia. *International journal of oncology*. 2016;48(4):1379-90. doi: 10.3892/ijo.2016.3359. PubMed PMID: 26820502.
81. Wang M, Kirk JS, Venkataraman S, Domann FE, Zhang HJ, Schafer FQ, Flanagan SW, Weydert CJ, Spitz DR, Buettner GR, Oberley LW. Manganese superoxide dismutase suppresses hypoxic induction of hypoxia-inducible factor-1alpha and vascular endothelial growth factor. *Oncogene*. 2005;24(55):8154-66. doi: 10.1038/sj.onc.1208986. PubMed PMID: 16170370.
82. Xia C, Meng Q, Liu LZ, Rojanasakul Y, Wang XR, Jiang BH. Reactive oxygen species regulate angiogenesis and tumor growth through vascular endothelial growth factor. *Cancer research*. 2007;67(22):10823-30. Epub 2007/11/17. doi: 10.1158/0008-5472.can-07-0783. PubMed PMID: 18006827.
83. Rigracciolo DC, Scarpelli A, Lappano R, Pisano A, Santolla MF, De Marco P, Cirillo F, Cappello AR, Dolce V, Belfiore A, Maggiolini M, De Francesco EM. Copper activates HIF-1alpha/GPER/VEGF signalling in cancer cells. *Oncotarget*. 2015;6(33):34158-77. doi: 10.18632/oncotarget.5779. PubMed PMID: 26415222; PMCID: PMC4741443.
84. Jiang F, Zhang Y, Dusting GJ. NADPH oxidase-mediated redox signaling: roles in cellular stress response, stress tolerance, and tissue repair. *Pharmacological reviews*. 2011;63(1):218-42. Epub 2011/01/14. doi: 10.1124/pr.110.002980. PubMed PMID: 21228261.
85. Teixeira G, Szyndralewicz C, Molango S, Carnesecchi S, Heitz F, Wiesel P, Wood JM. Therapeutic potential of NADPH oxidase 1/4 inhibitors. *British journal of pharmacology*. 2016. Epub 2016/06/09. doi: 10.1111/bph.13532. PubMed PMID: 27273790.
86. Bedard K, Krause KH. The NOX family of ROS-generating NADPH oxidases: physiology and pathophysiology. *Physiological reviews*. 2007;87(1):245-313. Epub 2007/01/24. doi: 10.1152/physrev.00044.2005. PubMed PMID: 17237347.
87. Geiszt M, Kopp JB, Varnai P, Leto TL. Identification of renox, an NAD(P)H oxidase in kidney. *Proc Natl Acad Sci U S A*. 2000;97(14):8010-4. Epub 2000/06/28. doi: 10.1073/pnas.130135897. PubMed PMID: 10869423; PMCID: PMC16661.
88. Helmcke I, Heumuller S, Tikkanen R, Schroder K, Brandes RP. Identification of structural elements in Nox1 and Nox4 controlling localization and activity. *Antioxidants & redox signaling*. 2009;11(6):1279-87. Epub 2008/12/09. doi: 10.1089/ars.2008.2383. PubMed PMID: 19061439.

89. von Lohneysen K, Noack D, Hayes P, Friedman JS, Knaus UG. Constitutive NADPH oxidase 4 activity resides in the composition of the B-loop and the penultimate C terminus. *The Journal of biological chemistry*. 2012;287(12):8737-45. Epub 2012/01/27. doi: 10.1074/jbc.M111.332494. PubMed PMID: 22277655; PMCID: PMC3308764.
90. Kawahara T, Ritsick D, Cheng G, Lambeth JD. Point mutations in the proline-rich region of p22phox are dominant inhibitors of Nox1- and Nox2-dependent reactive oxygen generation. *The Journal of biological chemistry*. 2005;280(36):31859-69. Epub 2005/07/05. doi: 10.1074/jbc.M501882200. PubMed PMID: 15994299.
91. Li YN, Xi MM, Guo Y, Hai CX, Yang WL, Qin XJ. NADPH oxidase-mitochondria axis-derived ROS mediate arsenite-induced HIF-1alpha stabilization by inhibiting prolyl hydroxylases activity. *Toxicology letters*. 2014;224(2):165-74. Epub 2013/11/06. doi: 10.1016/j.toxlet.2013.10.029. PubMed PMID: 24188932.
92. Meng D, Mei A, Liu J, Kang X, Shi X, Qian R, Chen S. NADPH oxidase 4 mediates insulin-stimulated HIF-1alpha and VEGF expression, and angiogenesis in vitro. *PloS one*. 2012;7(10):e48393. Epub 2012/11/13. doi: 10.1371/journal.pone.0048393. PubMed PMID: 23144758; PMCID: PMC3483150.
93. Mondol AS, Tonks NK, Kamata T. Nox4 redox regulation of PTP1B contributes to the proliferation and migration of glioblastoma cells by modulating tyrosine phosphorylation of coronin-1C. *Free radical biology & medicine*. 2014;67:285-91. Epub 2013/11/19. doi: 10.1016/j.freeradbiomed.2013.11.005. PubMed PMID: 24239742.
94. Schroder K, Zhang M, Benkhoff S, Mieth A, Pliquett R, Kosowski J, Kruse C, Luedike P, Michaelis UR, Weissmann N, Dimmeler S, Shah AM, Brandes RP. Nox4 is a protective reactive oxygen species generating vascular NADPH oxidase. *Circulation research*. 2012;110(9):1217-25. Epub 2012/03/30. doi: 10.1161/circresaha.112.267054. PubMed PMID: 22456182.
95. Heppner DE, van der Vliet A. Redox-dependent regulation of epidermal growth factor receptor signaling. *Redox biology*. 2016;8:24-7. Epub 2016/01/02. doi: 10.1016/j.redox.2015.12.002. PubMed PMID: 26722841; PMCID: PMC4710793.
96. Roy K, Wu Y, Meitzler JL, Juhasz A, Liu H, Jiang G, Lu J, Antony S, Doroshow JH. NADPH oxidases and cancer. *Clinical science (London, England : 1979)*. 2015;128(12):863-75. Epub 2015/03/31. doi: 10.1042/cs20140542. PubMed PMID: 25818486.
97. Bonello S, Zahringer C, Belaiba RS, Djordjevic T, Hess J, Michiels C, Kietzmann T, Gorlach A. Reactive oxygen species activate the HIF-1alpha promoter via a functional NFkappaB site. *Arteriosclerosis, thrombosis, and vascular biology*. 2007;27(4):755-61. Epub 2007/02/03. doi: 10.1161/01.ATV.0000258979.92828.bc. PubMed PMID: 17272744.
98. Diebold I, Flugel D, Becht S, Belaiba RS, Bonello S, Hess J, Kietzmann T, Gorlach A. The hypoxia-inducible factor-2alpha is stabilized by oxidative stress involving NOX4. *Antioxidants & redox signaling*. 2010;13(4):425-36. Epub 2009/12/31. doi: 10.1089/ars.2009.3014. PubMed PMID: 20039838.

99. Diebold I, Petry A, Hess J, Gorlach A. The NADPH oxidase subunit NOX4 is a new target gene of the hypoxia-inducible factor-1. *Molecular biology of the cell*. 2010;21(12):2087-96. Epub 2010/04/30. doi: 10.1091/mbc.E09-12-1003. PubMed PMID: 20427574; PMCID: PMC2883952.
100. Helfinger V, Henke N, Harenkamp S, Walter M, Epah J, Penski C, Mittelbronn M, Schroder K. The NADPH Oxidase Nox4 mediates tumour angiogenesis. *Acta physiologica (Oxford, England)*. 2016;216(4):435-46. Epub 2015/10/30. doi: 10.1111/apha.12625. PubMed PMID: 26513738.
101. Hsieh CH, Shyu WC, Chiang CY, Kuo JW, Shen WC, Liu RS. NADPH oxidase subunit 4-mediated reactive oxygen species contribute to cycling hypoxia-promoted tumor progression in glioblastoma multiforme. *PloS one*. 2011;6(9):e23945. Epub 2011/09/22. doi: 10.1371/journal.pone.0023945. PubMed PMID: 21935366; PMCID: PMC3174133.
102. Li J, Wang JJ, Yu Q, Chen K, Mahadev K, Zhang SX. Inhibition of reactive oxygen species by Lovastatin downregulates vascular endothelial growth factor expression and ameliorates blood-retinal barrier breakdown in db/db mice: role of NADPH oxidase 4. *Diabetes*. 2010;59(6):1528-38. Epub 2010/03/25. doi: 10.2337/db09-1057. PubMed PMID: 20332345; PMCID: PMC2874715.
103. Przybylska D, Janiszewska D, Gozdzik A, Bielak-Zmijewska A, Sunderland P, Sikora E, Mosieniak G. NOX4 downregulation leads to senescence of human vascular smooth muscle cells. *Oncotarget*. 2016;7(41):66429-43. Epub 2016/09/23. doi: 10.18632/oncotarget.12079. PubMed PMID: 27655718.
104. Serrander L, Cartier L, Bedard K, Banfi B, Lardy B, Plastre O, Sienkiewicz A, Forro L, Schlegel W, Krause KH. NOX4 activity is determined by mRNA levels and reveals a unique pattern of ROS generation. *Biochem J*. 2007;406(1):105-14. Epub 2007/05/16. doi: 10.1042/bj20061903. PubMed PMID: 17501721; PMCID: PMC1948990.
105. Tanaka M, Miura Y, Numanami H, Karnan S, Ota A, Konishi H, Hosokawa Y, Hanyuda M. Inhibition of NADPH oxidase 4 induces apoptosis in malignant mesothelioma: Role of reactive oxygen species. *Oncology reports*. 2015;34(4):1726-32. Epub 2015/08/05. doi: 10.3892/or.2015.4155. PubMed PMID: 26238284.
106. Dewhirst MW, Cao Y, Moeller B. Cycling hypoxia and free radicals regulate angiogenesis and radiotherapy response. *Nature reviews Cancer*. 2008;8(6):425-37. Epub 2008/05/27. doi: 10.1038/nrc2397. PubMed PMID: 18500244; PMCID: PMC3943205.
107. Tellier C, Desmet D, Petit L, Finet L, Graux C, Raes M, Feron O, Michiels C. Cycling hypoxia induces a specific amplified inflammatory phenotype in endothelial cells and enhances tumor-promoting inflammation in vivo. *Neoplasia (New York, NY)*. 2015;17(1):66-78. Epub 2015/01/28. doi: 10.1016/j.neo.2014.11.003. PubMed PMID: 25622900; PMCID: PMC4309725.
108. Michiels C, Tellier C, Feron O. Cycling hypoxia: A key feature of the tumor microenvironment. *Biochimica et biophysica acta*. 2016;1866(1):76-86. Epub 2016/06/28. doi: 10.1016/j.bbcan.2016.06.004. PubMed PMID: 27343712.

109. Dewhirst MW. Relationships between cycling hypoxia, HIF-1, angiogenesis and oxidative stress. *Radiation research*. 2009;172(6):653-65. Epub 2009/11/26. doi: 10.1667/rr1926.1. PubMed PMID: 19929412; PMCID: PMC2790140.
110. Chen WL, Wang CC, Lin YJ, Wu CP, Hsieh CH. Cycling hypoxia induces chemoresistance through the activation of reactive oxygen species-mediated B-cell lymphoma extra-long pathway in glioblastoma multiforme. *Journal of translational medicine*. 2015;13:389. Epub 2015/12/30. doi: 10.1186/s12967-015-0758-8. PubMed PMID: 26711814; PMCID: PMC4693410.